A review of hydrogen storage for vehicular application and the determination of the effect of extraction boil-off

Herman Lafras Retief

B.Eng. (Mechanical) North-West University

Potchefstroom Campus

Dissertation submitted in partial fulfilment of the requirements for the degree of *Masters in Engineering* at the Potchefstroom Campus of the North-West University

Supervisor: Prof. Johan Markgraaff

Potchefstroom, April 2012

ABSTRACT

In this study a review was done on various hydrogen storage systems to determine which system shows the best potential for vehicular application. The main criteria used were storage capacity, availability, safety and a net energy analysis. It was concluded that cryogenic systems currently show the best potential, followed by metal hydride systems. Compressed hydrogen systems showed much less potential for vehicular application than either cryogenic or metal hydride systems.

From the review, boil-off was identified as the main limiting factor of cryogenic systems. An investigation was launched to evaluate the use of a nozzle for extraction[1] of hydrogen from a cryogenic storage system, specifically focussing on its effect on boil-off. The cryogenic storage cylinder was insulated by means of vacuum. A finite element analysis simulation was used for this investigation.

Results in the form of temperature distribution, heat flux and boil-off were obtained. The nozzle system had little influence on changes in temperature profiles; however it caused a massive increase in heat absorbed by means of conduction. It is shown that this heat absorption leads to a very sharp increase of boil-off. Not only does this compromise the storage capacity, but it leads to another potential problem: the boil-off of hydrogen results in a phenomenon called self-pressurization, which raises concern in terms of safety.

The thermal breach created by the nozzle compromises the whole sophisticated insulation system to such a degree that it may jeopardise the overall viability of the storage system. It is recommended that another type of extraction system be used for extraction of hydrogen from a cryogenic storage system.

---

1 Extraction refers to the process where hydrogen gas flows from within the cryogenic storage vessel via a nozzle to outside the vessel.

Keywords: Hydrogen storage review; Hydrogen storage; Vehicular application; Cryogenic hydrogen storage; Nozzle extraction system; Boil-off; Heat transfer; Thermal breach.

OPSOMMING

In hierdie studie is verskeie waterstofbergingsmetodes ondersoek om te bepaal watter een van die metodes die meeste potensiaal het vir gebruik in voertuie. Die hoofkriteria wat gebruik is, is stoorkapasiteit, beskikbaarheid, veiligheid en ’n energie analise. Die gevolgtrekking was dat kriogeniese waterstofberging tans die meeste potensiaal toon, gevolg deur metaalhidried stelsels. Saamgeperste waterstofstelsels toon baie minder potensiaal as kriogeniese - of metaalhidriedstelsels.

In die hersiening is gevind dat die afkook van waterstof die mees beperkende faktor is by kriogeniese waterstofbergingstelsels. ’n Studie is geloods om die effek van ’n mondstuk wat gebruik word vir die onttrekking[1] van waterstof, te bepaal. Die kriogeniese sisteem wat gebruik is in die studie is geïsoleer deur middel van vakuum. Die ondersoek aangaande die afkook van waterstof is deur middel van ’n eindige element simulasie uitgevoer.

Resultate in terme van temperatuurverspreiding, hittevloei en afkook van waterstof is verkry. Die mondstuk sisteem het ’n klein invloed op temperatuur profiele gehad, maar het ’n drastiese toename veroorsaak in die hoeveelheid hitte geabsorbeer deur die sisteem. Daar is gevind dat hierdie hitte ’n skerp toename in die afkook van waterstof veroorsaak. Hierdie probleem veroorsaak nie alleenlik dat die bergingskapasiteit beïnvloed word nie, dit lei tot ’n veiligheidskwessie genaamd self-samedrukking.

Die termiese breuk wat deur die mondstuk veroorsaak word, beïnvloed die gesofistikeerde isolasiesisteem in so ’n mate dat dit die lewensvatbaarheid van die algehele sisteem in gedrang bring. Daar word voorgestel dat ’n ander metode gebruik word vir die onttrekking van waterstof vanuit ’n kriogeniese waterstofbergingstelsel.

1 Onttrekking verwys na die proses waar waterstofgas vloei vanuit die kriogeniese bergingsvat deur middel van ’n spuitstuk tot buite die kriogeniese vat.

Sleutelwoorde: Waterstofberging ondersoek; Waterstofberging; Voertuig toepassing; Kriogeniese waterstofberging; Mondstuk onttrekkingstelsel; Afkook; Hitte-oordrag; Termiese breking.

DECLARATION

I, Herman Lafras Retief (Identity Number: 870227 5204 082), hereby declare that the work contained in this dissertation is my own work. Some of the information contained in this dissertation was acquired from various journal articles, text books etc. and have been referenced accordingly.

Initial & Surname

(April 2012)

Witness

ACKNOWLEDGEMENTS

I make use of this opportunity to acknowledge the following parties:

- First and most importantly I would like to thank the Lord Jesus Christ, my Provider of inspiration, courage, talent, capability and perseverance throughout this research. All the glory to God.

Philippians 4:13 ~ For I can do everything through Christ, who gives me strength.

- To my grandfather Pierre and grandmother Annetjie, it means the world for me to be able to visit you and be encouraged physically, but more importantly spiritually. May the Lord be by your side forever. God bless you.
- For all their love and support I thank my father Francois, my mother Jeanette and my brother Pierre. God bless you.
- To my beautiful girlfriend Deanne, thank you for your love, encouragement and inspiration. May God bless our future together.
- To my supervisor Professor Johan Markgraaff, thank you for all the input, guidance and inspiration in the past two years. It was an honour and privilege for me to learn from someone like you, may God bless your future.
- To HySA (Hydrogen South Africa) for the funding required for this research.
- A word of thanks to the Faculty of Mechanical Engineering for the past six years' training.
- To all my colleagues working on their masters degrees, thank you for the companionship in good and bad times, it is truly appreciated.
- To all my friends in Veritas, if it weren't for you I would not have been the man that I have become, thank you for that. May you always stay men in truth and may the Lord always be Master of your life.

CONTENTS

List of tables

List of Figures

Nomenclature

Symbol	Description
°C	Degrees Celsius
1-D	One dimensional
3-D	Three dimensional
Al	Aluminum
bar	101.3 kPa
CAD	Computer Aided Design
CH_2	Compressed Hydrogen
cm	Centimeter
D H	Diffusion coefficient
DOELDP	Department of Energy Learning Demonstration Project
EES	*Engineering Equation Solver ©1992-2011 Academic Commercial V8.874-3D*
E_{in}	Energy absorbed over control surface
E_{out}	Energy desorbed over control surface
FeTi	Iron-Titanium
h	Plank's Constant
h_1	Convection coefficient of liquid hydrogen
H_2	Hydrogen gas
h_4	Convection coefficient of ambient air
h_{fg}	Latent heat of evaporation of hydrogen
K	Kelvin
k	Boltzmann's constant
kg	Kilogram
kJ	Kilojoule
km	Kilometer
L	Length of cylinder section
LH_2	Liquid Hydrogen
M	Metal
m	Meter
m_dot	Mass flow
Mg	Magnesium
MgH_2	Magnesium Hydride
MH_2	Metal hydride
Min	Minimum
MJ	Mega Joule
mm	Millimeter
MPa	Mega Pascal

Symbol	Description
Psi	Pounds per square inch
Q	Heat transfer
R&D	Research and Development
r1	Inner radius of inner cylinder
r2	Inner radius of vacuum
r3	Outer radius of vacuum
r4	Outer radius of outer cylinder
S	Second
T	Component thickness
T1	Liquid hydrogen temperature
T4	Ambient air temperature
US DOE	United States Department of Energy
V	Volt
W	Watt
wt %	Weight percentage
π	Pi

1. Introduction

The global demand for sustainable energy has become a topic of very serious concern in the last decade. Not only is there a growing demand for cleaner energy, but as Figure 1 points out, the gross energy consumed annually is also increasing. According to Salameh (2002) energy experts predict that oil supplies will only meet the global demand until an energy gap develops between 2013 and 2020. This gap will have to be breached, which will result in massive capital investments in unconventional and renewable energy sources.

Nuclear, solar and hydrogen energy plants are becoming major energy sources in the 21st century, but even with significant improvements, it will probably not even supply 7% of the global energy needed in 2025, perhaps rising to 13% in 2050 (Salameh, 2002). According to De Oliveira Matias and Devezasa (2007), it is possible to identify a viable substitution for the non-solid fossil fuels in the form of alternative energies. The question that remains is certainly this: what scenario can be expected in future?

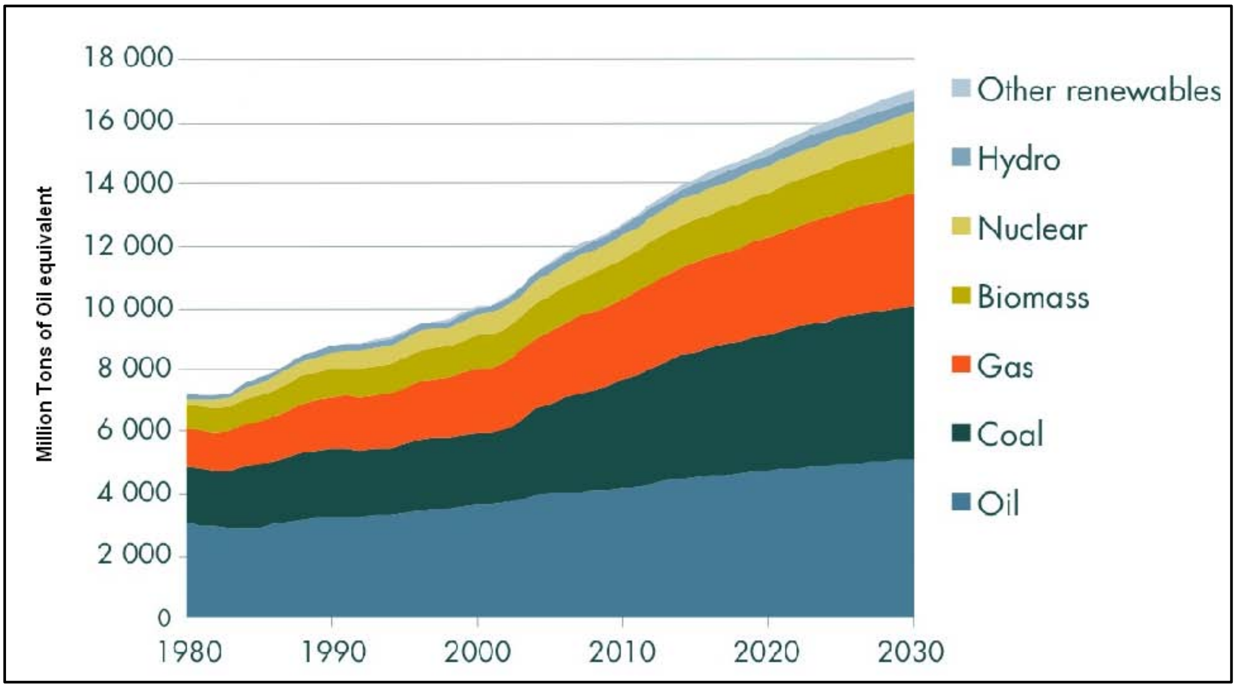

Figure 1: A graphical representation of the increasing global energy demand from 1980 to 2030

(Modified after In Situ Oil Sands Alliance, 2012).

Nuclear energy certainly seems viable, but predictions show that nuclear fusion as a commercial energy source will not be available before 2050-2060 (De Oliveira Matias

& Devezasa, 2007). According to Von Kaufmann (2004), using solar energy as an alternative is a highly ambitious approach. The reason for this is the very high initial cost of capital.

As an alternative to nuclear and solar energy, another form of energy exists. This energy is called hydrogen energy. Currently billions of dollars are being invested in hydrogen fuel cells and the hydrogen economy. This economy is mainly driven by the following key factors (Van Vuuren *et al.*, 2009):

- Concerns about energy security.
- The current rate of oil depletion.
- Environmental issues, in particular global warming.
- Deterioration of air quality of large cities (for example in Japan).
- The economic opportunities that the hydrogen economy may have in store.

The above-mentioned economic opportunities have lead to massive capital investments into the hydrogen economy. The drive behind these investments is the existence of a massive interest in hydrogen as energy carrier. The main reasons for this interest is that hydrogen is clean, the most abundant element in the universe, the lightest fuel and also has the richest energy per unit mass of about 142 MJ/kg (Bossel & Eliasson, 2003; Jain *et al.*, 2010). Another attracting fact about hydrogen energy is that hydrogen may be produced using a variety of energy sources, including renewable energy (Johnston *et al.*, 2005).

However, although hydrogen energy shows promising potential for use in vehicles, there are still a few hurdles to overcome in order to be a feasible substitute for current fossil fuel energy. One of these hurdles is hydrogen storage (Ahluwalia *et al.*, 2011). Hydrogen gas is very light, transparent and has a very low density at standard temperature and pressure. The low density makes storage of hydrogen a major challenge. It is a technical issue of such magnitude that the storage of hydrogen is the major bottleneck in the hydrogen vehicle program (Aceves *et al.*, 2000; Ho & Rahman, 2007a; Zhou, 2005).

When considering hydrogen as fuel for vehicular application, the importance of storage is clearly evident. Three types of hydrogen storage stations need to exist for the system to function. Firstly the hydrogen gas must be stored directly after hydrogen gas formation. Secondly, storage systems must be in place at refuelling stations and thirdly, it must be stored in the vehicle itself while it is on the move or stationary. This emphasizes the importance of effective storage methods for hydrogen, clearly indicating one of the challenges of using hydrogen as a fuel source.

Because of the large interest developing in the last two decades, the storage of hydrogen has received much attention. Many storage methods and systems have been developed and investigated, with promising results in some cases. Currently, the main storage systems include (Van Vuuren *et al.*, 2009):

- Compressed hydrogen.
- Cryogenic hydrogen storage systems.
- Metal hydrides.

Currently these systems are evaluated based on targets set by the USDOE (United States Department of Energy) where (in most cases) only the gravimetric and volumetric capacities are considered. Although the gravimetric and volumetric capacities are definitely two of the most important criteria for evaluating hydrogen storage systems, it does not consider the practical implications of using these systems. For instance, important matters like safety, material issues, hydrogen charge and discharge rates, automotive accidents and driving range are not considered.

This implies that only looking at storage capacity in the evaluation of a storage system for vehicular application is not sufficient, since using merely gravimetric and volumetric storage capacities only gives a vague idea of the true potential of a certain hydrogen storage system. This identified problem is supported by the research done by Ahluwalia *et al.* (2011) where hydrogen storage options were evaluated for both on-board as well as off-board performance. It may therefore be necessary to include a more extensive range of criteria when considering the viability of different hydrogen storage methods.

2. Problem statement and aim

In the evaluation of the viability of hydrogen storage methods, using only storage capacity as criteria is not sufficient. The true viability and potential of a hydrogen storage system will only be made evident by a thorough review where a broader spectrum of criteria is included.

The aim of this study is twofold. Firstly it is to review hydrogen storage systems for use in vehicular application. Secondly the aim is to further investigate the most promising storage method and its associated technological pitfalls.

3. Literature Survey

3.1 Storage capacities and targets

In this section the current status of various storage systems is evaluated. Two of the most important criteria for measuring storage capability are the volumetric and gravimetric capacity of the system. Volumetric capacity refers to the mass of hydrogen per unit system volume (measured in gram per litre). Gravimetric capacity refers to the mass of hydrogen per unit system mass. It is a dimensionless indicator of the relation between the mass of hydrogen and the total system mass (Sarkar & Banerjee, 2004).

The volumetric and gravimetric capacities of various storage systems are shown in Table 1. Comparing systems with a hydrogen weight percentage of 100%, liquid and solid storage systems show much more potential in terms of volumetric capacity than pressurized hydrogen. Magnesium hydride (MgH_2) shows the most potential among the metal hydrides. It has a weight percentage of 7.6% hydrogen, as well as a high volumetric capacity relative to other hydrides.

Table 1: Volumetric and gravimetric hydrogen capacities for various storage systems (Jain *et al.*, 2009).

Material	**H-atoms per cm^3 (x10e22)**	**Weight % hydrogen**
H_2 gas, 200 bar (2850 psi)	0.99	100
H_2 liquid 20 K (-253°C)	4.2	100
H_2 solid 4.2 K (-269°C)	5.3	100
MgH_2	6.5	7.6
Mg_2NiH_4	5.9	3.6
$FeTiH_{1.95}$	6	1.89
$LaNi_5H_{6.7}$	5.5	1.37
$ZrMn_2H_{3.6}$	6	1.75
VH_2	11.4	2.1

In a graphical comparison of storage methods, it is evident from Figure 2 that metal hydrides and liquid hydrogen are in the lead in terms of volumetric capacity. Because of its very low volumetric and low gravimetric capacity, compressed gas storage systems show much less potential for hydrogen storage in vehicles than metal hydrides and cryogenic storage systems (Ahluwalia *et al.*, 2011).

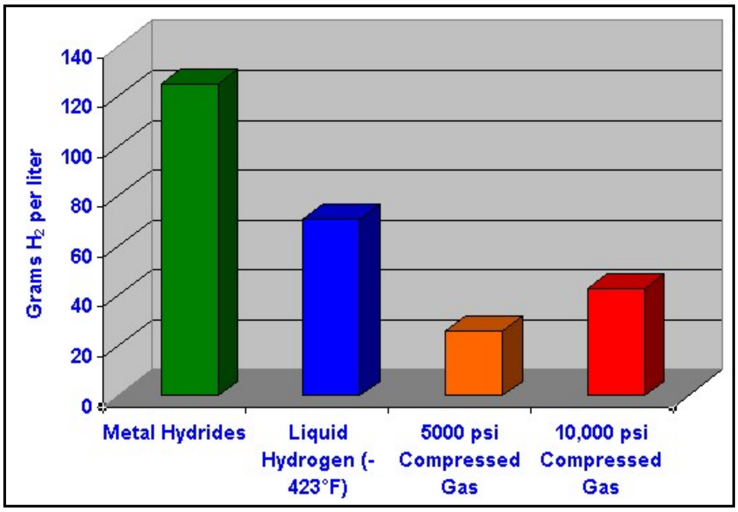

Figure 2: Graphical comparison of storage methods in terms of hydrogen density (Modified after Anon, s.a.).

However, before any further investigation can be done, storage targets need to be set. The minimum viable amount of hydrogen gas that needs to be stored for vehicular application is about 5 kg. In terms of energy this is equivalent to about 19 litres of gasoline. This estimation is made based on a general-purpose vehicle that provides a range of 640 km in a 34 km/litre hybrid or fuel cell vehicle. Storing this amount of hydrogen in the form of compressed gas will fill a volume so big that it would be difficult to use in light-duty cars. If hydrides are used, the total storage system would weigh in excess of 305 kg (with 5 kg being hydrogen), depending on the type of hydride used (Aceves *et al.*, 2000).

To get a broad perspective of current and future storage targets, the targets set in 2009 by the USDOE (United States Department of Energy) are presented in Table 2 (Dillich, 2009). This table is used as a base to evaluate storage capacities of different storage methods. For ultimate storage targets, a gravimetric density of 7.5 weight percentage is required, whilst maintaining a volumetric density of at least 70 grams per litre.

Table 2: Performance targets of hydrogen storage systems as revised in 2009 by the USDOE (Dillich, 2009).

Target	**2010**		**2015**		**Ultimate**
	Old	**New**	**Old**	**New**	**New**
System gravimetric density [% wt.] (kWh/kg)	6 (2.0)	4.5 (1.5)	9 (3.0)	5.5 (1.8)	7.5 (2.5)
System volumetric density [g/L] (kWhr/L)	45 (1.5)	28 (0.9)	81 (2.7)	40 (1.3)	70 (2.3)
System fill time for 5kg fill [minutes] (kg H_2/minute)	3 (1.67)	4.2 (1.2)	2.5 (2.0)	3.3 (1.5)	2.5 (2.0)
System cost [$/kg$H_2$] ($/kWhrnet)	133 (4)	133* (4)*	67 (2)	67* (2)*	tbd
*Cost targets are still being considered as other H2-fuel cell vehicle targets are assessed.					

Data from the United States DOELDP (Department of Energy Learning Demonstration Project) shows that although current storage systems, especially cryogenic systems, are approaching the 2010 targets, it is quite clear that none of the current systems meet both gravimetric and volumetric targets for 2015. It should also be kept in mind that other factors such as cost, charging and discharging rates and durability also contribute to the feasibility of the final system (Dillich, 2009; Satyapal *et al.*, 2007).

In the next section, a more detailed perspective of hydrogen storage systems is presented.

3.2 A review of storage methods

As was concluded from Figure 2 above, the use of metal hydrides and cryogenic storage systems show much more potential than compressed gas systems for use in vehicular application due to its higher volumetric and gravimetric properties. It is for this reason that only two storage types will further be investigated: the use of metal hydrides, followed by cryogenic storage systems.

3.2.1 Metal hydrides

A hydride can be defined as a compound of hydrogen with another, more electropositive element or group (The American Heritage Dictionary, 2000). A metal hydride is thus a compound of hydrogen with a metal such as lithium. The principle of storing hydrogen in the form of metal hydrides lies in the ability of certain metals to form a chemical compound consisting of large quantities of hydrogen under certain conditions.

Currently, one of the most promising metal hydrides is magnesium hydride (MgH_2). The reason for it being continually and intensely investigated is that it has a high gravimetric capacity of 7.6 wt. % hydrogen and a volumetric capacity of ~85 kg/m^3. It is also inexpensive relative to other hydrides, offering potential for storage of hydrogen for automobile applications (Pourpoint *et al.*, 2010). Its use is impeded mainly by the fact that it has a very high desorption temperature (in the region of 300°C or higher) for normal atmospheric pressures.

Another impeding factor is the kinetics of diffusion of hydrogen throughout the material. The diffusion of hydrogen throughout a layer of magnesium is extremely slow (~10^{-17} cm^2/s at room temperature) (Alonso, 2010). The slow rate of diffusion leads to another problem. It influences the formation of stoichiometric MgH_2 meaning that the maximum storage capacity may not be reached. Not only does the diffusion of hydrogen influence the storage capacity, it may cause another substantial problem. Under a certain set of circumstances it is possible that a layer of MgH_2 may form on the outer surface of the magnesium. This drastically slows the diffusion of hydrogen through the storage media, until for a certain critical layer thickness, diffusion stops totally (Jain *et al.*, 2009).

The resulting effect is thus not only that the storage media is not a total hydride; but that another very important concern arises: a nucleus of pure Mg is formed. Pure Mg has the potential to oxidize spontaneously at about 2,500 K (Champagne *et al.*, 2008) which gives rise to very serious safety issues.

Further intense research and development (R&D) is needed to modify the properties and conditions of absorption and desorption of hydrides if they are to become viable. The aim is to modify the material in such a manner that it falls within the operating range of temperature and pressure set by the USDOE (Jain *et al.*, 2009). The optimum scenario is to utilize waste heat from available sources such as a power plant or waste engine heat for the operation of the storage system (Heung, 2003).

In order to address the problem of diffusion, another research approach was taken. The use of thin films was considered for hydrogen storage. The storage of hydrogen in Mg-based thin films is very much related to storage in bulk metal hydrides. The film consists of one or more metallic layers with the ability to absorb hydrogen under certain conditions. A saturated hydrogen content as high as 5.5 wt. % at 298 K and 70 kPa can be reached (Jianglan, 2009).

Advantages of thin films include alloying with other metals resulting in a reduced desorption energy and enthalpy of formation (Barcelo *et al.*, 2010). Disadvantages include a reduction in storage capacity (Barcelo *et al.*, 2010), poor sorption kinetics (Tan *et al.*, 2009), possible oxidation (Barcelo *et al.*, 2010), film buckling and detachment and flaking (Pranevicius *et al.*, 2009). Thus, although thin films show more potential than bulk magnesium hydrides in the form of lower desorption energy, a net energy analysis indicates that the major drawback in MgH_2 thin films remains the high desorption temperature (Sarkar & Banerjee, 2004). This indicates that the same thermodynamic issue of the total energy associated with hydrogen desorption still exists. The use of catalyst materials has the ability to reduce this desorption energy, but it reduces the storage capacity.

Another very important criterion in analyzing a hydrogen storage system is energy requirement. A study by Sarkar *et al.* (2004) showed that magnesium hydride storage systems consume 3001 kJ for a one kilometre ride. This total is the sum of three contributors. The direct energy required to travel is 1,164 kJ, while the energy required for producing and storing hydrogen totals 1,777 kJ. The energy required to produce the tank is 60 kJ. Results from this study show that hydrides consume more energy (in the form of hydrogen) per kilometre travelled than cryogenic storage systems. This is due to the combined effect of the greater mass of the tank and the energy associated with hydrogen desorption (Sarkar & Banerjee, 2004).

In terms of availability of fuel, the use of a magnesium hydride storage system raises concern. Not only is there the possibility of the formation of non-stoichiometric hydrides, another problem is that metal hydrides are associated with slow hydrogen uptake and release kinetics (Satyapal *et al.*, 2007). This means that hydrogen will not always be available immediately as required under certain conditions.

Considering the mentioned advantages and disadvantages it is concluded that the main storage limitation of magnesium hydride is the energy required for desorption, while the main attraction towards this type of storage is the high volumetric capacity (Barcelo *et al.*, 2010; Pourpoint *et al.*, 2010).

3.2.2 Cryogenic storage systems

In this section the use of cryogenic storage systems is examined. The term cryogenic may be defined as the branch of physics concerned with the provision of environments of very low temperatures and the phenomena occurring at these temperatures (Collins English Dictionary, 2009). Cryogenic hydrogen storage thus implies that the hydrogen is cooled down to a point where it liquefies. This phenomenon is known as condensation. In this liquefied state the properties of hydrogen changes such that the storage of hydrogen in this form has the potential to become viable.

Liquid hydrogen is in the order of 840 times denser than hydrogen gas. This implies that the transformation from gaseous to liquid hydrogen makes massive improvements on both volumetric and gravimetric storage capacities. A cryogenic hydrogen storage system's volumetric capacity is in the order of 0.036 kg per litre (mass hydrogen per unit system volume) while its gravimetric capacity is 0.14 kg per kg (mass hydrogen per unit system mass). Consequently, it is concluded that although not yet at a totally satisfactory level, these capacities show very promising possibilities.

However, to realise these possibilities, cryogenic hydrogen storage systems must first overcome a few hurdles. Liquefying hydrogen gas requires about 36.6 MJ/kg (Satyapal *et al.*, 2007). The temperature range for liquefaction is about 15 to 20 Kelvin (about -258 to -253°C). This implies that all materials used should be able to function at these extreme temperatures. Another consideration to make in terms of liquid hydrogen is the expansion of hydrogen from 20 Kelvin to its critical point at 33 Kelvin. It is for this reason that liquid hydrogen tanks are only filled to 85-95% of their capacity. If this 5-15% space is not empty, hydrogen spillage may occur (Ahluwalia & Peng, 2008).

Another major challenge, and most probably the single biggest concern and limitation in cryogenic applications, is hydrogen boil-off (Ahluwalia & Peng, 2008; Ho & Rahman, 2007b; Jorgensen, 2010). In short, boil-off may be defined as the vaporization of liquid (The American Heritage Dictionary, 2000). Hydrogen boil-off is a result of the phase change from liquid to gaseous hydrogen due to the absorption of energy from the environment. In order to prevent boil-off, the energy level within the liquid hydrogen should be kept below an energy level known as the latent heat of evaporation of liquid hydrogen.

The key to successfully storing hydrogen in a cryogenic state is thus to minimize the energy transfer to the liquid hydrogen, or better yet, eliminate it completely. But, how can this be done?

One option is the use of high efficiency insulation, since it is known that insulation is the main factor affecting boil-off (Li *et al.*, 2004).Technology has made it possible to manufacture insulated cryogenic tanks with extremely low heat transfer (in the order of 1-3 W) (Van Vuuren *et al.*, 2009). Although this number is very low, evaporative losses remain a massive issue in cryogenic hydrogen storage because of the massive temperature difference between ambient conditions and liquid hydrogen (Incropera *et al.*, 2007). In the case where a cryogenic storage system is used in a vehicle, the hydrogen needs to be vented after about 3-5 days of inactivity. For longer periods of inactivity, all of the hydrogen may be lost due to evaporation, possibly leaving the driver stranded (Ahluwalia & Peng, 2008).

In an attempt to eliminate the boil-off losses of traditional cryogenic systems, another type of cryogenic storage system was developed. These systems are called cryogenic-capable pressure vessels, meaning that the hydrogen is stored in a pressure vessel that can operate at cryogenic temperatures (about 20 Kelvin) and high pressures (e.g. 350 atm). This vessel can be filled either with liquid hydrogen, compressed gaseous hydrogen or with cryogenic hydrogen at elevated supercritical pressures, namely cryo-compressed hydrogen. The broad range of storage parameters makes this system more flexible, enabling it to make use of the advantages of both liquid hydrogen and compressed gaseous hydrogen.

When using cryogenic-capable pressure vessels, the implication is that it has the ability to contain either liquid hydrogen or compressed gaseous hydrogen. The energy levels associated with liquid hydrogen is in the order of 3.25 kWh/kg, while the energy level of compressed hydrogen gas is only 1.75 kWh/kg. However, temperatures in the range smaller than 20 Kelvin is required to keep hydrogen in a liquefied state, while compressed hydrogen systems operate at normal ambient temperatures of about 300 Kelvin.

The highlighted area shown in Figure 3 indicates the range in which the combined system can operate.

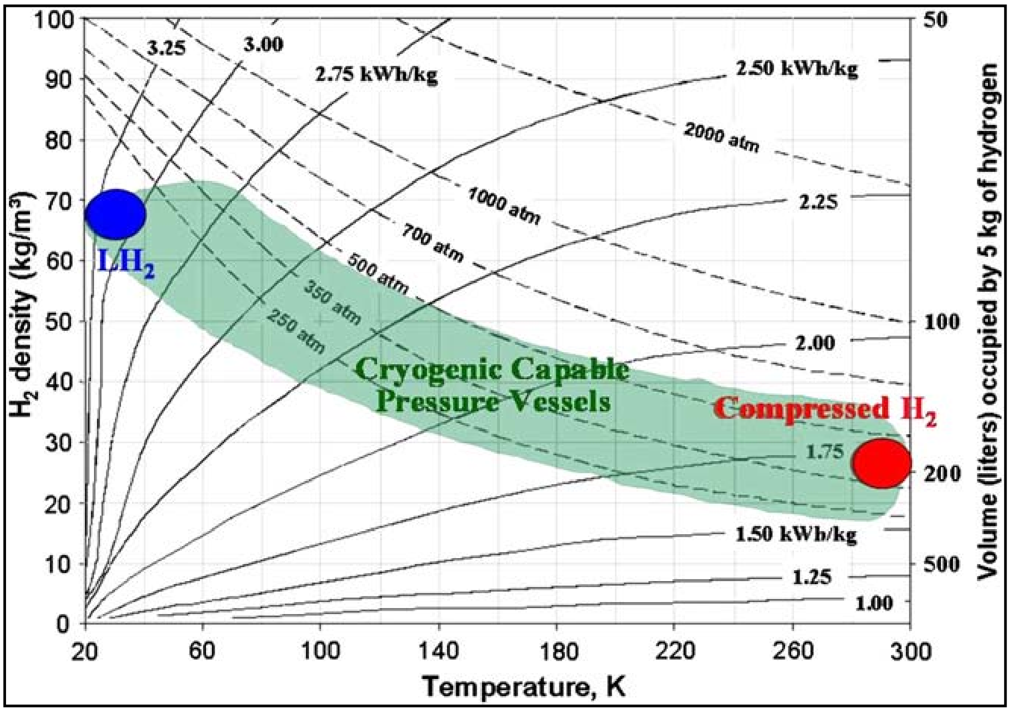

Figure 3: The storage range of cryogenic capable pressure vessels in terms of temperature, volume and hydrogen density (Aceves *et al.*, 2009).

Advantages of insulated pressure vessels include material benefits, lower evaporative losses and a higher gravimetric storage capacity than metal hydrides (Aceves *et al*., 2000). In a study by Ahluwalia *et al.* (2008), cryogenic H_2 storage in an insulated pressure vessel was investigated. It was found that, for a tank that can manage 350 bar, the evaporative losses cannot deplete H_2 from the tank beyond 64% of the theoretical storage capacity. This means that the cryo-compressed system has an advantage over traditional cryogenic hydrogen storage systems.

The use of a combined system thus looks very promising, but this system also has its drawbacks. Since this system combines the advantages of two separate systems, it also combines the disadvantages. Although a slight change is made in the method of storage and the system, the same problems in terms of boil-off still exist.

It should also be noted that these systems have a few problems of their own. When using a system of cryogenic compressed liquid hydrogen, other issues include the total electrical energy needed to compress the hydrogen gas at elevated temperatures, the possibility of a decrease of storage density, the limited capacity of hydrogen tube trailers and also the capital cost of infrastructure capable of handling hydrogen at these conditions (Ahluwalia & Peng, 2008).

In terms of safety, the use of cryogenic hydrogen storage systems has (among others) one substantial safety issue namely self-pressurization. Because of the nature of the gaseous form of hydrogen, the formation of hydrogen gas causes a pressure rise within the system (Seo & Jeong, 2010). This implies that at some stage, hydrogen has to either be consumed or it will be lost to the environment. This is particularly an issue for vehicles being inactive in confined spaces such as parking garages (Satyapal et al., 2007).

One of very few upsides to boil-off is, because of the effect of self-pressurization, that the hydrogen is readily and immediately available as required by the system. However, this one positive side effect of boil-off does not come close to compromising for the massive negative effect of hydrogen loss due to boil-off.

Apart from the volumetric capacity, gravimetric capacity, availability and safety considerations, the final criterion used for evaluation is a net energy requirement. It was shown that a vehicle using a cryogenic storage system uses 2,956.3 kJ to travel one kilometre. This is the sum of the direct energy required to travel, the energy required to produce and store the hydrogen and the energy required to produce the tank. These factors consume 768 kJ, 2,172.7 kJ and 15.6 kJ respectively (Sarkar & Banerjee, 2004). The total energy consumed is slightly lower than that of the magnesium hydride storage system; however the magnitude of this difference is negligibly small.

3.3 Review summary and discussion

With the advantages and disadvantages of both magnesium hydride and cryogenic storage systems known at this stage, the question that needs to be answered is this: Which one of these two systems is currently deemed best for use in vehicular application? In this section, this question is addressed. The criteria selected for evaluation are volumetric capacity, gravimetric capacity, availability, a net energy analysis and safety considerations.

Table 3: A comparison between cryogenic hydrogen storage and metal hydride storage of hydrogen.

	Cryogenic storage	**Mg hydride storage**
Volumetric capacity-Mass of H_2 per unit system volume (kg/l) (Tan *et al.*, 2009)	0.036	0.081
Gravimetric capacity-Mass of H_2 per unit system mass (kg/kg) (Tan *et al.*, 2009)	0.14	0.025
Total energy required for a 1 km drive (kJ)	2,956.3	3,001
Availability	Hydrogen gas immediately available.	Due to slow uptake and release kinetics hydrogen may not always be available immediately.
Safety considerations	Continuous evaporation generates gaseous hydrogen which results in an increase in pressure inside a liquid hydrogen storage vessel if not properly released.	Under certain circumstances a nucleus of pure Mg may form. Pure Mg has the potential to oxidize spontaneously at about 2500 K, a very serious safety issue.

A comparison of the advantages and disadvantages of cryogenic and metal hydride storage of hydrogen is presented in Table 3. Magnesium hydride tanks lead the way in terms of a per volume basis, but on a per weight basis they perform poorly. Cryogenic hydrogen storage systems fulfil both criteria (Sarkar & Banerjee, 2004). Since these two factors are the most important criteria, another comparison was made. This was done by comparing the two systems for the storage of 5 kg hydrogen (as it is the assumed theoretical minimum required for vehicular application). In order to store 5 kg of hydrogen, a cryogenic storage system would weigh about 40 kg, compared to a magnesium hydride tank of almost 230 kg. However, it should be kept in mind that the same cryogenic tank will occupy about 0.14 square meters, compared to only 0.06 square meters required by the magnesium hydride storage system.

Although both systems have potential safety issues, none of the issues is of a magnitude that it compromises any of the two systems as a whole.

The magnesium hydride system poses a problem in the sense that it is not able to immediately deliver hydrogen gas as it is required. Cryogenic storage systems do not have this problem, since they can provide high pressure hydrogen gas under most conditions due to the self-pressurization effect of boil-off.

Energy usage of both systems is in the range of 3,000 kJ, indicating that the two storage systems draw level in terms of a net energy analysis.

Thus the question about which system is the best for vehicular application still remains unanswered. To answer it, the main consideration is the requirements of the vehicle. For general storage purposes the use of either cryogenic or Mg-hydride storage systems for storing hydrogen seems viable. However, in terms of vehicular application, there are two important requirements: system weight and availability.

For vehicular application, the gravimetric capacity of a storage system carries more weight than the other factors, especially in modern light weight vehicles. Considering that modern light weight vehicles weigh in the order of 800 kg, the 190 kg difference in weight between the cryogenic tank and the hydride tank is considerable. It should also be kept in mind that future legal standards may add more pressure on weight reduction of vehicles (Van den Biggelaar, 2010).

The second important factor is availability. According to Satyapal *et al.* (2007), the current issue with the immediate availability of hydrogen gas is of such magnitude that using metal hydrides for vehicular application is not feasible. A cryogenic system has the ability to supply fuel as it is required with much more ease than a metal hydride system (Ho & Rahman, 2007a).

It is because of their gravimetric capacity and immediate availability of hydrogen gas that cryogenic storage systems are considered to have more potential than Mg-hydride systems when it comes to vehicular application. In conclusion, based on this review, cryogenic storage systems are currently the most promising option for storing hydrogen for use in vehicular application.

As mentioned in the aim of this study, once the most promising storage method is identified, it will be evaluated in more depth in terms of its technological pitfalls.

From the review it is evident that the biggest limitation of cryogenic storage systems is boil-off. But this problem has been addressed by many investigators by improvements made to insulation performance and application (Van Vuuren *et al.*, 2009; Li *et al.*, 2004).

However, although insulation performance is certainly one of the most important factors affecting boil-off, one other major problem still exists. Keeping in mind that the aim of the system is to eventually deliver hydrogen for use in a vehicle, the extraction thereof poses a substantial problem (Van Vuuren *et al.*, 2009). In this context, extraction simply refers to the process where the hydrogen flows from within the storage system to the outside, making it available for combustion. Extraction is usually done by using some sort of nozzle or fluent carrier. In cryogenic hydrogen storage systems the nozzle used in the extraction process creates a thermal breach. Even with sophisticated high technology insulation, this breach allows for relatively large amounts of heat to be transferred into the system, resulting in the loss of hydrogen gas due to the phenomenon called boil-off.

This problem is also mentioned in a study by BMW, where the cryo-compressed hydrogen storage concept was investigated (Aceves *et al.*, 2009). In another study by Kumar *et al.* (2010), sharp temperature gradients were observed in the refuelling process, but the effect thereof on boil-off was not investigated.

4. Investigation Purpose and Objectives

From the previous section it is concluded that limited quantitative information is available on the effect of hydrogen extraction on boil-off of cryogenic hydrogen storage.

The purpose of this investigation is therefore to obtain a better understanding of the issues involved in extraction of hydrogen and its effect on overall insulation and boil-off losses. Due to limited resources and available experimental facilities this issue was addressed by applying heat transfer calculation models supplemented by an associated finite element thermal modelling approach.

The objectives of this investigation are to:

- Set up an analysis setup and procedure which includes the determination of system dimensions, material properties and boundary conditions.
- Perform a series of steady state FEA's on the storage system in order to be able to determine the heat flow into the system for different conditions.
- Determine a mathematical correlation between heat flow and boil-off for this specific system.
- Use this mathematical correlation, in conjunction with heat flow results from the FEA, to determine the effect of a nozzle on boil-off for different conditions.
- Interpret the investigation results relative to one another.
- Make logical conclusions and recommendations.

5. Boil-off Calculation

To achieve the purpose of the study the following approach was followed. It started with the determination of the storage model assembly and the calculation of related dimensions. From this the creation of a virtual CAD (Computer Aided Design) model was realized. The CAD model was then used to set up a thermal circuit on which heat transfer calculations were carried out. This was done to determine the heat flow into the system as well as the corresponding boil-off of hydrogen.

This chapter also includes a finite element thermal analysis, based on the assumptions previously discussed, inclusive of the assumed boundary conditions.

In the following section the determination of the dimensions and assembly of the CAD model are given.

5.1 CAD Model assembly and dimensions

The model used for the heat transfer calculations and FEA simulations is an assembly consisting of four parts. These parts are the outer cylinder, the vacuum space, the inner cylinder that holds the cryogenic fluid and a nozzle used for hydrogen gas extraction. Detailed drawings of the inner cylinder, vacuum and outer cylinder are presented in drawing numbers 1, 2 and 3 respectively in Appendix A.

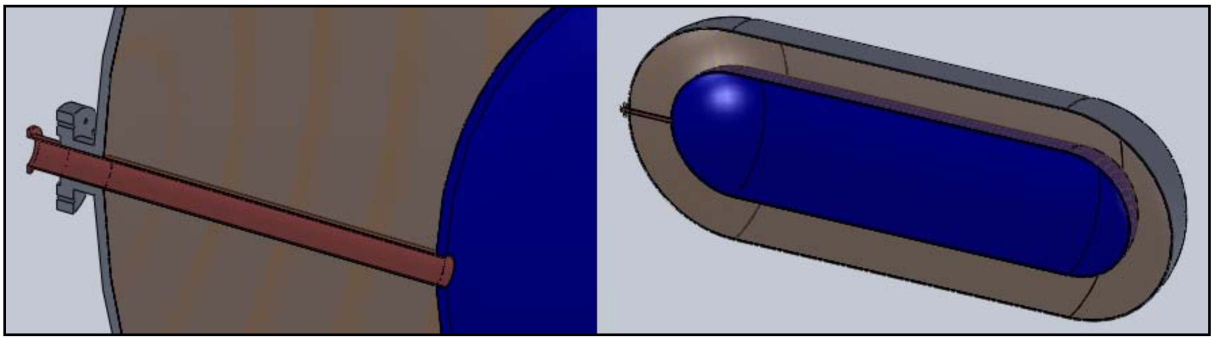

Figure 4: A section cut of the CAD model showing the four parts of the model.

As indicated by the section cut of the model in Figure 4, the core of the model is the inner cylinder, surrounded by the vacuum. The design of the vacuum space is such that there is a fixed distance between the inner and outer cylinders at any position. The outer cylinder forms a shell around the vacuum. At one end of the outer cylinder provision is made for a feed tube. The tube has a flange on the end for the purpose of support and attachment to the outer cylinder. The nozzle (feed tube) is positioned concentrically in the outer cylinder header.

The use of the correct dimensions for this model is critical, since it influences both the volumetric and gravimetric capacities of the storage system. In the next paragraph, the calculation of the system's dimensions is presented.

The first step was to determine the inner cylinder capacity (volume). This was done by using the energy value per kilogram for both gasoline and hydrogen. These values were used to determine that two hydrogen tanks containing hydrogen worth 700 MJ of energy each will be adequate for use in vehicular application. However, only one tank was evaluated for this study. The total required volume of the inner tank was calculated based on liquid hydrogen density. Solving equations simultaneously for the volume of a sphere and a cylinder, the inner radius of the inner tank were determined, from which the other dimensions were calculated.

Table 4: CAD model dimensions as calculated manually.

Calculated CAD Model dimensions	
Total system length [m]	1.1
Inner cylinder inner radius [m]	0.15
Inner cylinder outer radius [m]	0.153
Outer cylinder inner radius [m]	0.25
Outer cylinder outer radius [m]	0.253
Cylinder wall thickness [m]	0.003
Inner cylinder volume [m^3]	0.07

Results from the above-mentioned calculations are presented in Table 4. The CAD model used in this study was then created using these dimensions. Details of the calculations are presented as EES (*Engineering Equation Solver)* Code Section 1 and Solution Section 1 in Appendix C.

5.2 Heat Transfer – Manual calculations

The dimensions obtained in the previous section were then used in a mathematical model to calculate the heat transfer and boil-off. This model is based on calculations of Incropera *et al.* (2007), where the boil-off of liquid nitrogen from an insulated tank was determined. Equations were set up manually using first principle heat transfer methods. The equations were solved using *Engineering Equation Solver © 1992-2011 Academic Commercial V8.874-3D* (EES).

The manual calculations were divided into two tasks. The first task was to find the rate of heat transfer to the liquid hydrogen as further explained below in paragraph 5.2.1. The second task consisted of using results obtained in the first task to determine the rate of hydrogen gas boil-off. The second task is explained in paragraph 5.2.3.

5.2.1 Calculation of the rate of heat transfer

The calculation of heat transfer was based on a composite wall of different materials, experiencing a temperature difference between the outer surfaces. In order to set-up the mathematical model, a number of assumptions were made. The assumptions for this analysis were that:

- Steady state conditions exist.
- One dimensional transfer in the radial direction occurs.
- Material properties remain constant throughout the entire calculation.
- Negligible radiation exchange between the outer surface of the outer cylinder and the surroundings occurs.
- Negligible radiation between the inner surface of the outer cylinder and the outer surface of the inner cylinder.

For calculation purposes the CAD model was divided into two separate sections. The one section was the cylinder part of the tank, while the other section was the remaining two halved spheres, as indicated below in Figure 5. The two halved spheres were then considered as one total single sphere for calculation purposes. The advantage of using this approach is that two simple systems could be solved simultaneously, rather than considering the system as a single and more complex entity.

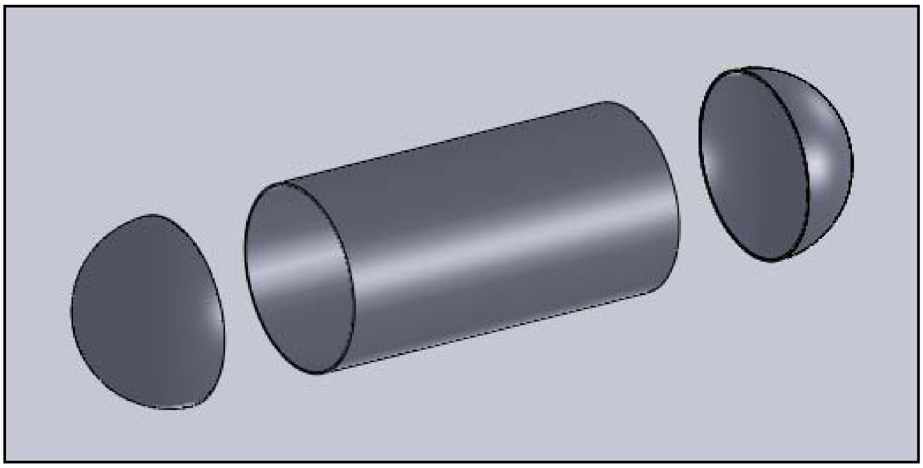

Figure 5: A graphical representation of the virtual model used for manual calculations.

For both the sphere and cylinder a thermal circuit that involves conduction and convection was created. Details of the assumptions made are further discussed in paragraph 5.2.2.

5.2.2 Assumptions

The thermal resistance in terms of conduction and convection are given by the following standard equations:

For radial conduction in a cylinder:

$$Rt = \frac{\ln\left[\frac{r1}{r2}\right]}{2Lk\pi}$$

For radial convection in a cylinder:

$$Rt = \frac{1}{2h\pi L(r1)}$$

For radial conduction in a sphere:

$$Rt = \frac{1}{4k\pi} \times \left[\frac{1}{r1} - \frac{1}{r2}\right]$$

For radial convection in a sphere:

$$Rt = \frac{4\pi r^2}{h}$$

with:

r1 = inner radius [m]

r2 = outer radius [m]

h = convection heat transfer coefficient [W/m^{2}K]

k = conduction heat transfer coefficient [W/mK]

L = length of the cylinder [m]

Using the above equations, a thermal circuit was set up as a composite cylinder and sphere wall consisting of three planes. This circuit was used to calculate conduction through the walls, whilst convection occurred on the inner and outer surfaces of the storage system. This circuit is graphically represented below in Figure 6. The calculations used to solve the thermal circuit are based on a combination of five individual heat transfer zones evident from the circuit. Each of these sections was considered to be a thermal resistor. The circuit provides for convection on both ends of the thermal circuit (indicated by A and E), while the inner three sections (B, C and D) indicate the sections where conduction occurs.

In order to determine the total resistance within the circuit, a heat transfer equation for both the cylinder and the sphere had to be obtained. Consequently the total heat transfer was calculated by dividing the temperature difference of the two fluids by the total thermal resistance within the thermal circuit.

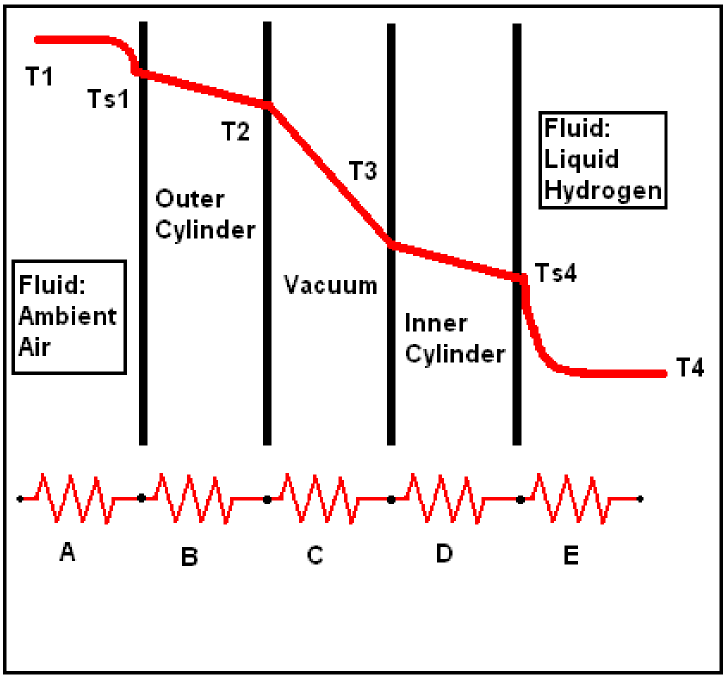

Figure 6: Schematic of the thermal circuit used for calculations in EES.

Based on the discussed principles, the following equation was set-up for heat transfer through the cylinder incorporating both convection and conduction:

$$Net\ heat\ flow\ through\ cylinder = \frac{T1 - T4}{A + B + C + D + E}$$

where:

$$A = \frac{1}{2 \times \pi \ \times L \times r1 \times h1}$$

$$B = \frac{\ln\left(\frac{r2}{r1}\right)}{2 \times \pi \times L \times [k(Outer\ cylinder)]}$$

$$C = \frac{\ln\left(\frac{r3}{r2}\right)}{2 \times \pi \times L \times [k(Insulation)]}$$

$$D = \frac{\ln\left(\frac{r4}{r3}\right)}{2 \times \pi \times L \times [k(Inner\ cylinder)]}$$

$$E = \frac{1}{2 \times \pi \ \times L \times r4 \times h4}$$

The following equation was set up for heat transfer through the sphere incorporating both convection and conduction:

$$Net\ heat\ flow\ through\ sphere = \frac{T1 - T4}{F + G + H + I + J}$$

where:

$$F = \frac{1}{h1 \times 4 \times \pi \times r1^2}$$

$$G = \frac{1}{4 \times \pi \times [k(Inner\ cylinder)]} \times \left(\frac{1}{r1} - \frac{1}{r2}\right)$$

$$H = \frac{1}{4 \times \pi \times [k(Insulation)]} \times \left(\frac{1}{r2} - \frac{1}{r3}\right)$$

$$I = \frac{1}{4 \times \pi \times [k(Outer\ cylinder)]} \times \left(\frac{1}{r3} - \frac{1}{r4}\right)$$

$$J = \frac{1}{h4 \times 4 \times \pi \times r4^2}$$

With:

r1 =inner radius of inner cylinder [m]

r2 = inner radius of vacuum [m]

r3 = outer radius of vacuum [m]

r4 = outer radius of outer cylinder [m]

h1 = convection coefficient of liquid hydrogen [kJ/kgK]

h4 = convection coefficient of ambient air [kJ/kgK]

T1 = liquid hydrogen temperature [K]

T4 = ambient air temperature [K]

The heat transfer results from the cylinder and sphere were totaled to obtain the amount of heat that was absorbed by the system. Results from the first part of the manual calculations thus yielded a value of heat transfer into the system, however the amount of boil-off resulting because of it was not known. In the next section, the calculation for the rate of boil-off is discussed.

5.2.3 Calculation of the rate of hydrogen boil-off

The rate of hydrogen boil-off was determined by performing an energy balance for a control surface around the liquid hydrogen. For this setup, if follows that:

$$\mathbf{E_{in} - E_{out} = 0}$$

The value $\mathbf{E_{in}}$ is equivalent to the rate of heat transfer to the liquid hydrogen. The mode of calculation of the value of $\mathbf{E_{in}}$ was presented in the previous paragraph. The value $\mathbf{E_{out}}$ is associated with the gain of latent energy due to boiling of the hydrogen. This value was calculated using the following equation:

$$Eout = m_{dot} \times h_{fg}$$

where:

$$Eout = \ rate\ of\ heat\ transfer\ [W]$$

$$m_{dot} \ = mass\ flow\ [\frac{kg}{second}]$$

$$h_{fg} \ = latent\ heat\ of\ evaporation\ [\frac{kJ}{kg}]$$

Because the rate of heat transfer to the liquid hydrogen is equal to the loss of latent heat due to evaporation, this equation was used to calculate the mass flow of boil-off over time. Manipulation of the derived equation showed that the boil-off rate of hydrogen was equal to the quotient of the heat transfer and the latent heat of evaporation. From this knowledge it was calculated that the boil-off of the system is a linear function of the amount of heat flow over the system boundary. For the system used in this study, this relates to a linear function such that for a daily heat flow of one Watt over system boundary, the related daily boil-off of hydrogen is 1.93 kg.

5.3 Heat transfer - Finite element analysis

From the previous section it was evident that it is possible to calculate the amount of boil-off manually, however results were limited to numerical values. Another issue with the results was that it did not give any insight into local heat transfer, heat flux and temperature profiles. This indicated that results obtained from manual calculations are limited to a certain degree.

The use of a finite element analysis simulation software package would allow the analysis of very complex geometries. Such simulation software would also provide more insight into heat flux, temperature distribution and heat flow in the form of both numerical and graphical results. It also has the ability to parameterize material properties and boundary conditions. This function allows the user to rapidly alternate the simulation for various conditions.

The finite element analysis (FEA) simulation package that was used is ANSYS. It is an industry standard FEA simulation software package, which has the capacity to evaluate the effect of the nozzle system by using various input parameters.

5.3.1 The storage system

In order to use ANSYS to simulate heat transfer, a virtual 3-D CAD storage system was modeled in SolidWorks® 2010, with the dimensions as given in Table 4. Model parts were generated in SolidWorks® 2010 and assembled to provide a virtual model as a base for the simulation. Interference detection was done to ensure the optimal model for heat transfer simulations. The virtual storage system files were then imported into ANSYS for the purpose of simulation, followed by a very important editing process. The editing process was necessary to edit existing materials in the ANSYS library, ensuring that the correct thermal properties were applied and used during the simulation process.

5.3.2 Meshing

An important part in a finite element analysis is the meshing and associated meshing controls. For this study, two considerations were made. Firstly, the type of mesh and its associated parameters were selected. Secondly the selection of the appropriate element size was performed by means of a mesh independence study. In this section these two considerations are explained shortly.

ANSYS generally uses either a free mesh or a mapped mesh. A *free mesh* has no restrictions in terms of element shapes, and has no specific pattern applied to it. A *mapped mesh* is restricted in terms of the element shape it contains and the pattern of the mesh.

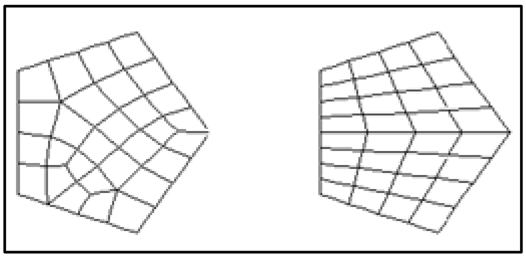

Figure 7: A schematic showing the two types of mesh that ANSYS generally uses. On the left is an example of free mesh, while the right hand side gives an example of mapped mesh.

For this study, an ANSYS setting called DESIZE was used to produce a free mesh. Although a mapped mesh would have worked for most of the surfaces and volumes on the model, a free mesh was chosen because it can easily accommodate the sharp edges and changes in geometry in the nozzle area.

In the setting DESIZE a number of element sizes were controlled based on recommendations of the 2009 ANSYS Modelling and Meshing guide for a standard heat transfer simulation. The following settings were made:

MINL Minimum number of elements that will be attached to a line when using lower order elements. MINL was set to 3 elements per line.

MINH Minimum number of elements that will be attached to a line when using higher-order elements. MINH was set to 2 elements per line.

MXEL Maximum number of elements that will be attached to a single line (lower or higher order elements). MXEL was set to 15 elements per line for h-elements and 6 divisions per line for p-elements. (An h-element is the normal type of element that ANSYS used before revision 5.1, while the p-element is a slightly faster and more accurate element used since revision 5.1). For this simulation a default combination of h- and p-elements were used.

ANGL Maximum spanned angle per lower-order element for curved lines. ANGL was set to 15 degrees per element.

ANGH Maximum spanned angle per higher-order element for curved lines. ANGH was set to 28 degrees per element.

EDGMN Minimum element edge length. EDGMN was set to the minimum possible edge length. It should be considered that MINL or MINH argument can override this value.

EDGMX Maximum element edge length. EGDMX was set to the maximum possible edge length. It should once again be considered that the MXEL argument can override this value.

ADJF Target aspect ratio for adjacent line used for free meshing. Was set to 1.0, which attempts to create equal sided h-elements; defaults to 4 for p-elements.

The second consideration in terms of meshing was the selection of the appropriate mesh element size. A very fine mesh would give very accurate results, but is associated with very long computational time. The goal of this analysis was thus to determine an acceptable element size that would result in the shortest possible computational time, while the analysis still maintained acceptable accuracy.

This selection of an appropriate mesh element size was performed by means of a mesh independence study. This implied that the FEA model was solved with progressively smaller mesh sizes until a negligibly small change in the results for a smaller mesh size was observed. At this stage it was argued that the results were independent of the mesh size, thus mesh independency was obtained. Tabular and graphical results for the mesh independency study on the model used for this study are shown in Table 5 and Figure 8 respectively.

Table 5: Results obtained from the mesh independency study showing the amount of heat transfer associated with different mesh element sizes.

Element size [mm]	**Heat transfer [W]**
20	1.46254
15	1.47646
10	1.48389
5	1.48399
2	1.48398

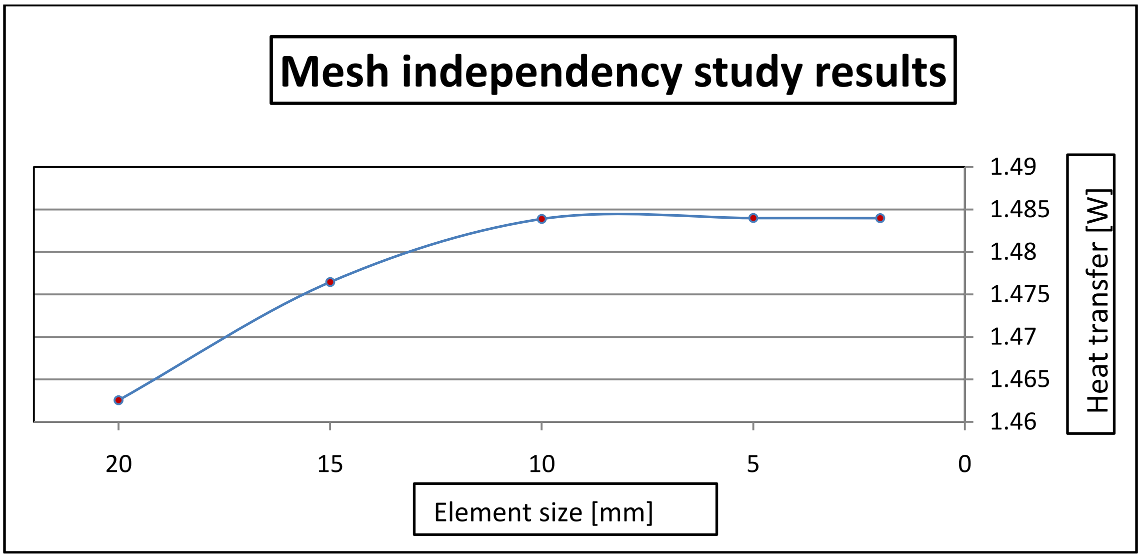

Figure 8: A graphical representation of results of the mesh independency study.

The first observation is that there are two main sections on the graph. The first part is the section from 20 mm to 10 mm element size where larger (a total difference of 0.02135 W) differences in results are observed. The second section is from 10 mm to 2 mm. Since there is a negligibly small difference (total difference of 0.0001 W) in results in this section, it indicates that mesh independency was reached at an element size of 10 mm for this study. Therefore an element size of 10 mm was selected for meshing in this investigation.

5.3.3 Assumptions

Similar to manual calculations carried out or conducted, the following assumptions apply to the ANSYS modeling. These assumptions are reviewed and discussed below.

- **Effective thermal conductivity**

  In terms of heat transfer, an effective thermal conductivity is used as representative of the overall heat transfer within the system. According to Van Antwerpen (2009) the effective thermal conductivity is a summation of various components of the overall heat transfer and can be used to calculate heat transfer using this single thermal conductivity value. This assumption is also supported by the use of an equivalent thermal conductivity for cryogenic calculations (Incropera *et al.*, 2007).

- **Perfect insulation**

  In the development of the virtual 3-D storage system a section cut was incorporated into the design as indicated in Figure 9. This was done so that it would be possible to have access to and to view the whole system throughout the analysis. The implication of this section cut was that the analyzed model now had more surfaces exposed to ambient conditions than it was supposed to have. These extra surfaces had to be perfectly insulated; otherwise ambient conditions would have a non-realistic impact on the analysis.

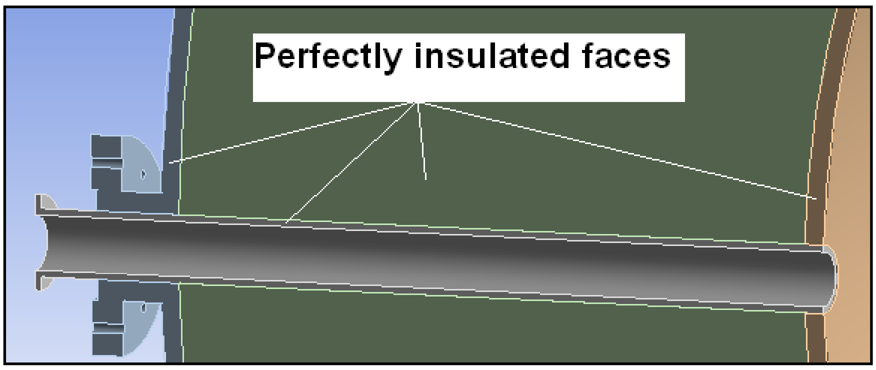

Figure 9: A representation of the four perfectly insulated faces for purposes of simulation.

It was assumed that the perfect insulation of these faces had such a small impact on heat transfer calculations that the effect thereof could be neglected.

- **Weld seams**

  It was assumed that the manufacturing of all components is of such a nature that all joints are perfectly smooth with no evidence of weld seams or any irregularities.

- **Suspension of inner cylinder**

  Another assumption that was made is that the inner cylinder is simply balanced in the center of the total storage system with no contact with the outer cylinder.

- **Suspension of outer cylinder**

  The suspension for the outer tank is not included in this study. The assumption made here is that the effect of heat transfer caused by the support or suspension of the outer cylinder is incorporated into the convection coefficient on the outer surface.

- **Leaks**

  It is assumed that there are no leaks in the system. This is for both heat leaks and hydrogen leaks in the nozzle vicinity.

- **Nozzle connection**

  The connection between the nozzle and the inner cylinder is a 100% fit. It is a simple, smooth sliding connection that is not composed of any thread or any other connecting mechanism.

- **Ambient conditions**

  It was assumed that ambient conditions are constant throughout the entire simulation, except in one case where the aim of the test was to evaluate the effect of different ambient temperatures.

- **Convection within the system**

  Another assumption made is that there is no forced convection within the gases and liquids both on the inside and on the outside of the system. The only convection to be considered by the simulation code is free convection.

- **Thermal effects**

  It was also assumed that the effects of any other thermal phenomena are negligibly small in comparison with the effects of heat transfer and thermal strain.

- **Constant heat transfer coefficients**

  All heat transfer coefficients used in this simulation were assumed to be constant throughout the entire simulation, thus implying that the thermal heat transfer coefficients are not temperature dependent.

5.3.4 Boundary conditions and values

With the assumptions made, there were two final input parameters left to be assigned, being convection and conduction constants and the selection of ambient temperature. In the next two paragraphs, the selection of these parameters is explained.

The following selections were made:

- For both the inner and outer cylinders, the selected material was 316L stainless steel which according to standard date has an average thermal conductivity of 16.2 W/mK. The inner and outer cylinder thermal conductivity used was 16 W/mK.
- For the isolation (or vacuum), a very low thermal conductivity value of 0.0002 W/mK was assigned for simulation. This is in line with the findings of Incropera *et al.* (2007), where an evacuated foil-mat blanket with a thermal conductivity value of only 0.00016 W/mK was proposed for cryogenic applications.
- The latent heat of evaporation value of liquid hydrogen is 44.6 kJ/kg (UIG, 2007).
- Convection constants for ambient air and liquid hydrogen were set at 20 $W/m^2.K$ and 90 $W/m^2.K$ respectively (Incropera *et al.*, 2007).

- For the nozzle material, the thermal conductivity value used for evaluation was 5 W/mK. This value is based on results from an analysis done using the CES (Cambridge Engineering Selector). CES is a software package that makes use of an extensive database of information to assist designers in material driven decisions. The detail on the selection process is given in Appendix D.

The ambient temperature was set at 26°C for all simulations, except in the case where the effect of a change in ambient temperature was investigated. The choice for this value was based on findings by MAN Diesel, where the influence of ambient temperatures on engine operation was investigated (MAN Diesel, 2010).

5.3.5 Simulation procedure

In order to run the simulation, a graphical user interface of ANSYS namely Workbench Release 13.0 was used to import the CAD model and set up the thermal model. A detailed simulation procedure and report are given in Appendix B.

For the investigation of any condition, for example the influence of ambient temperature, a series of simulation runs was completed in order to obtain perspective of its effect on boil-off. In most cases, the series consisted of about ten steady state simulation runs. For each following run, the value of the parameter under investigation was changed to obtain results for the altered condition, while the rest of the parameters remained unchanged.

For every simulation series the results were gathered manually. Simulation results are given in the next chapter.

6. Heat transfer and boil-off results

After completing the simulation setup and procedure successfully, results were obtained from ANSYS. In the first part of this chapter, results directly related to the nozzle are given, followed by results concerning the effect of secondary systems on boil-off.

For clarity reasons the following definitions are given:

Base model: The base model is defined as the model without the extraction nozzle. It consists of only an inner and outer cylinder with the vacuum space between the two cylinders.

Extraction model: The extraction model is defined as the model consisting of the exact same parts as the base model, but also includes a nozzle.

In the final section of this chapter the simulation results are evaluated and verified.

It is important to take note that this chapter only explains the setup used to obtain the results, as well as the relevant results obtained. Chapter seven focuses on the discussion of the results.

6.1 The effect of hydrogen extraction with a nozzle

6.1.1 Heat flux

In terms of heat flux, the base model showed a maximum heat flux of about 0.9 W/m² at the spherical ends of the storage system. The heat flux into the cylindrical part of the inner tank is between 0.4 W/m² and 0.6 W/m². The heat flux for the model without an extraction nozzle is shown in Figure 10.

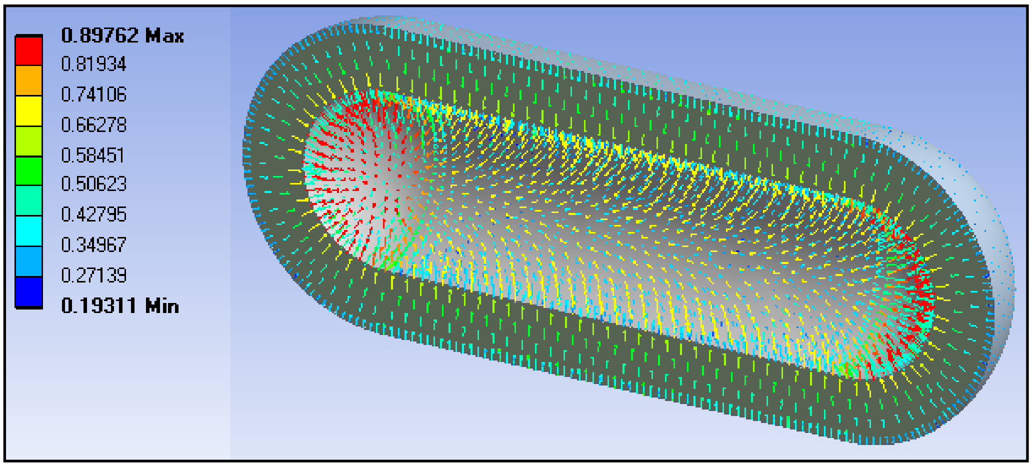

Figure 10: Vector representation of the heat flux [W/m^2] into the base model.

For the extraction model the heat flux takes on a very different shape. It is evident from Figure 11 that the heat flux is concentrated in the nozzle area, with the maximum heat flux being above 18,000 W/m². Although the vectors indicating heat flux for the rest of the model still exist, they are so small in comparison with that flowing through the nozzle area that they cannot be seen.

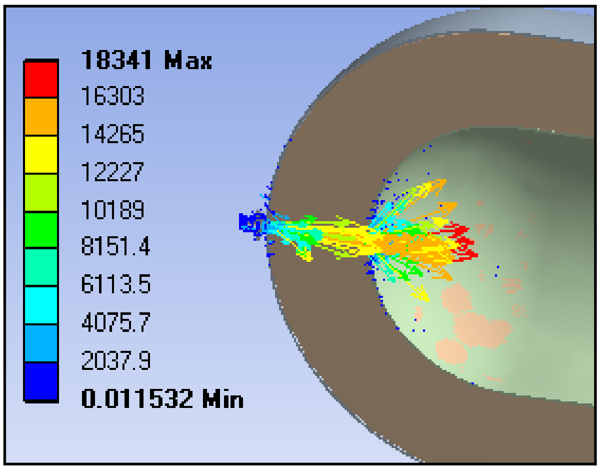

Figure 11: Vector representation of the heat flux [W/m^2] into the storage cylinder model as caused by a nozzle system.

6.1.2 Temperature and temperature profiles

Results obtained from the ANSYS simulations show that the maximum temperature on the outer cylinder of the base model was 26°C, while the effect of the nozzle caused a rise in maximum temperature to 27.3°C on the outer surface of the extraction model. This effect can be seen in Figure 12 and Figure 13.

An unexpected observation is that the temperature profile is shaped towards the outside along the nozzle. As mentioned the observed results will be explained in the following chapter.

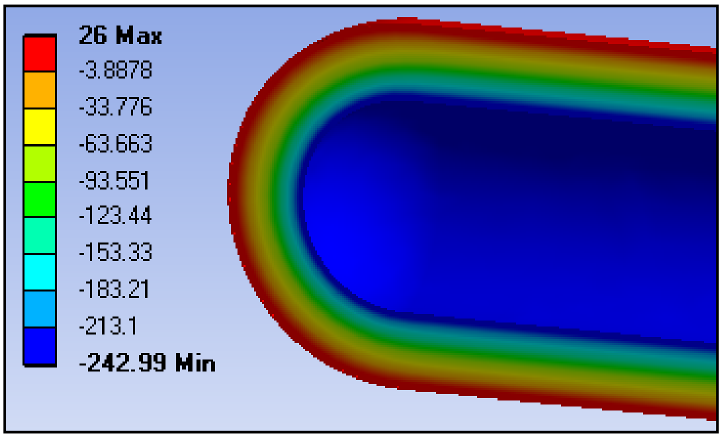

Figure 12: A graphical representation of the temperature distribution [°C] through a system without a nozzle.

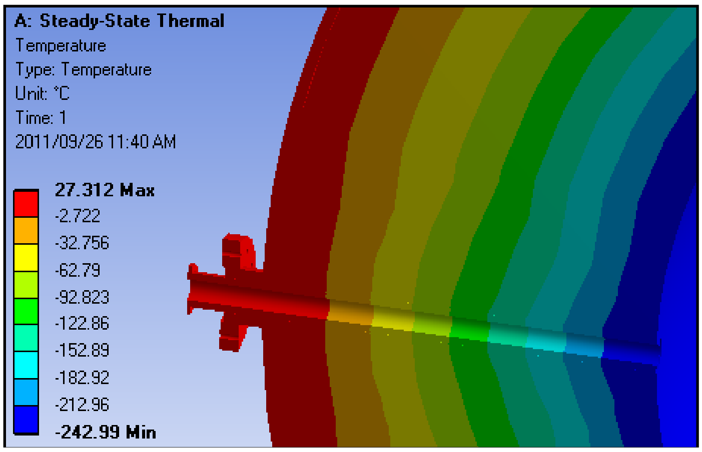

Figure 13: A graphical representation of the temperature distribution [°C] in the vicinity of the nozzle.

6.1.3 Heat flow and related boil-off

The most important result of the investigation is the effect of the nozzle on boil-off. These results show the difference in boil-off between the base model and the extraction model. Results in terms of heat flow and related boil-off are given in Table 6, which is the single most important result of the investigation. In the right hand column the hydrogen lost due to boil-off is compared to an equivalent volume of gasoline.

Table 6: The difference in boil-off between a model without a nozzle compared to a model with a nozzle.

Model	Heat flow [W]	Hydrogen Boil-off [kg/day]	Equivalent amount of gasoline lost per day [liter]
Base value	0.77	1.498	6.73
With nozzle	1.484	2.877	12.96
Difference	0.714	1.379	6.23

It is firstly noticed that a base value of 0.77 Watt exists. This important observation shows that even for the model without a nozzle, boil-off still exists.

It is evident that the hydrogen boil-off nearly doubles as a result of the nozzle extraction system for this set of conditions. In terms of the equivalent volume of gasoline lost per day, the difference between the base model and a model with a nozzle is a massive 6.23 liters of gasoline lost daily due to boil-off.

6.2 The effect of different nozzle dimensions

In the following simulations the extraction model was used continuously, but small changes were made in the dimensions of the nozzle to determine the effect thereof on heat flow. Four systems with different nozzles were simulated for this evaluation. Detailed schematics of the nozzles used for this investigation are presented in Appendix A. The outer diameters of the nozzles were considered to be a constant, while the inner diameter was reduced and corresponding total nozzle wall cross-sectional area was reduced incrementally. A section cut showing the geometry of the first nozzle used for evaluation is shown in Figure 14.

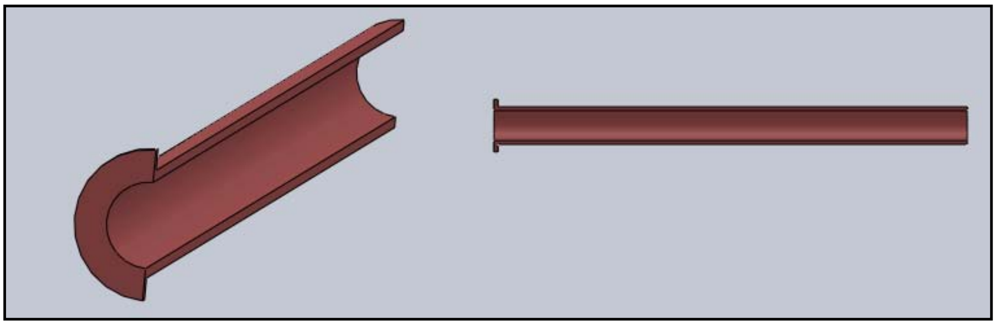

Figure 14: A section cut, showing the basic geometry of the nozzle used for evaluation of the effect of nozzle dimensions on heat flow.

Results in terms of nozzle wall thickness, total nozzle wall cross-sectional area and heat flow are given in Table 7.

Table 7: The effect of different nozzle dimensions on the heat absorbed by the system.

Nozzle no.	OD [mm]	Wall thickness [mm]	Total nozzle cross sectional area [mm^2]	Heat flow [W]
1	10	2	50.64	1.48396
2	10	1.5	40.06	1.35754
3	10	1	28.28	1.14660
4	10	0.5	14.92	1.00334

The first observation made from the results is that the total nozzle area has a profound effect on the heat flow into the system. For a reduction of 75% of the wall thickness, a reduction of about 33% of heat flow is observed. Secondly it is observed that the reduction of total nozzle cross-sectional area is not related to a linear reduction of the heat flow into the system.

6.3 The effect of the thermal conductivity of the nozzle

In this section the thermal conductivity of the nozzle was varied to determine the effect thereof on heat transfer. This was done by simulating two sets of simulations where the thermal conductivity of the nozzle was changed incrementally. The first set of simulations evaluated the effect between 1 W/mK and 21 W/mK in increments of 4 W/mK. Results for this set are given in Table 8 and Figure 15. The second set evaluated smaller heat conducting values varying from 0.2 W/mK to 1.2 W/mK in increments of 0.2 W/mK. For these increments, the results are given in Table 9 and Figure 16.

Table 8: The effect on heat flow into the system due to the variation of the thermal conductivity of the nozzle between 1 W/mK and 21 W/mK.

Thermal conductivity value [W/mK]	Total heat flow into the system [W]
1	0.92808
5	1.48396
9	2.0116
13	2.521
17	3.016
21	3.5016

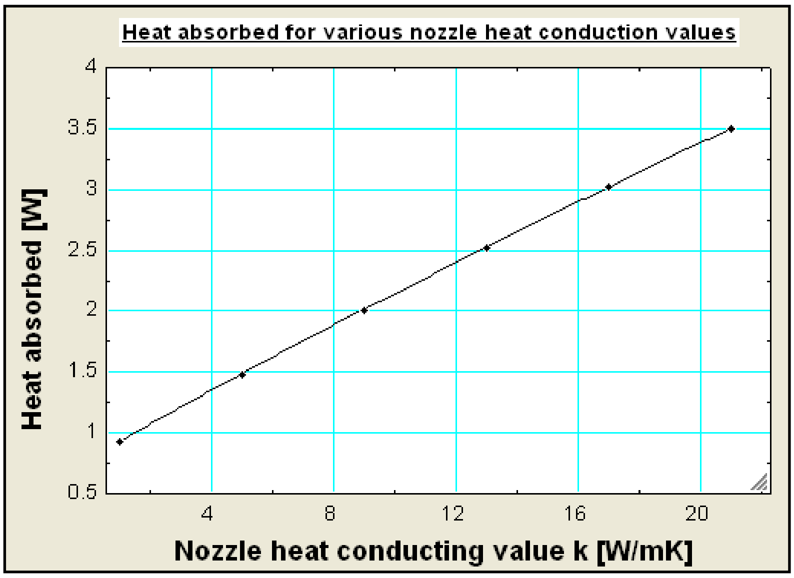

Figure 15: The relation between the heat absorbed and the nozzle heat conducting value for increments from 1 W/mK to 21 W/mK.

It is observed that for a low thermal conductivity value of only 5 W/mK, the heat transferred is already 1.484 W, meaning that an additional 0.714 W has entered the system (in comparison with the base model). Although it seems like a very small amount of energy transferred, it is responsible for about half of the total heat flow, and thus also responsible for the same portion of boil-off.

For a thermal conductivity value of 21 W/mK, the total amount of heat flow that the nozzle contributes is about 3.57 times the amount of a system without a nozzle. This is a total of roughly 2.75 W, corresponding to a boil-off of about 0.21 kg hydrogen per hour.

Table 9: The effect on heat flow into the system due to the variation of the thermal conductivity of the nozzle between 0.2 W/mK and 1.2 W/mK.

Thermal conductivity value [W/mK]	Total heat flow [W]
0.2	0.80814
0.4	0.83906
0.6	0.86916
0.8	0.8988
1	0.92808
1.2	0.9571

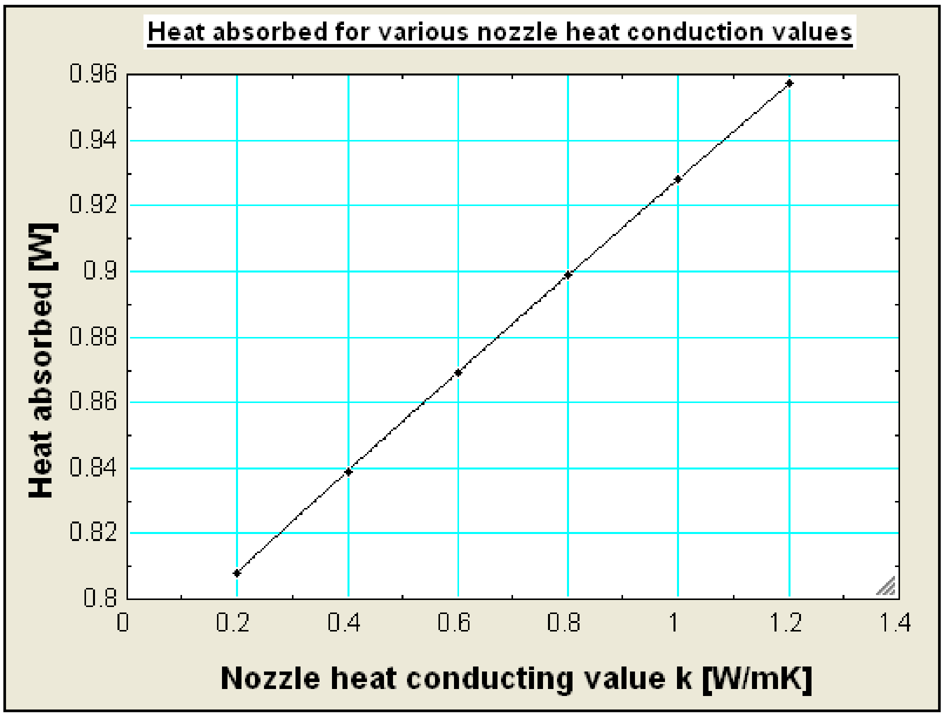

Figure 16: The relation between the amount of heat absorbed and the nozzle heat conducting value for increments between 0.2 W/mK and 1.2 W/mK.

6.4 The effect of secondary systems on heat flow

In this section the effect of secondary components within the system were evaluated. This means that although a nozzle is permanently included in the simulation, the focus is not on the nozzle but rather on the secondary components listed below. The reason for the evaluation of secondary components is to determine their effect on heat flow and boil-off.

In the next three paragraphs the setup and results for each component evaluation are given.

The components evaluated for this purpose are:

- The inner and outer cylinder thermal conductivity.
- The thermal conductivity of the vacuum.
- The effect of ambient temperature on the system.

6.4.1 Variation of thermal conductivity of the cylinder material

In this section the effect of the thermal conductivity of the inner and outer cylinder material was investigated. The same thermal conductivity was assigned to both cylinders.

A total of nine simulations were performed in two sets. For the first set of simulations, the thermal conductivity values varied from 20 W/mK to 100 W/mK with increments of 20 W/mK. The corresponding thermal energy absorbed is presented in Table 10 and Figure 17. A second set of simulations were also performed to determine the heat flow at very low thermal conductivity values. Increments of 5 W/mK were used to simulate the system between 5 W/mK and 20 W/mK. Parameters and results are given in Table 11 and Figure 18.

Table 10: Energy absorbed for different heat conductivity values of the cylinders for increments from 20 W/mK to 100 W/mK.

Cylinder thermal conductivity value W/mK]	Energy absorbed [W]
20	1.49194
40	1.51836
60	1.5357
80	1.54928
100	1.56074

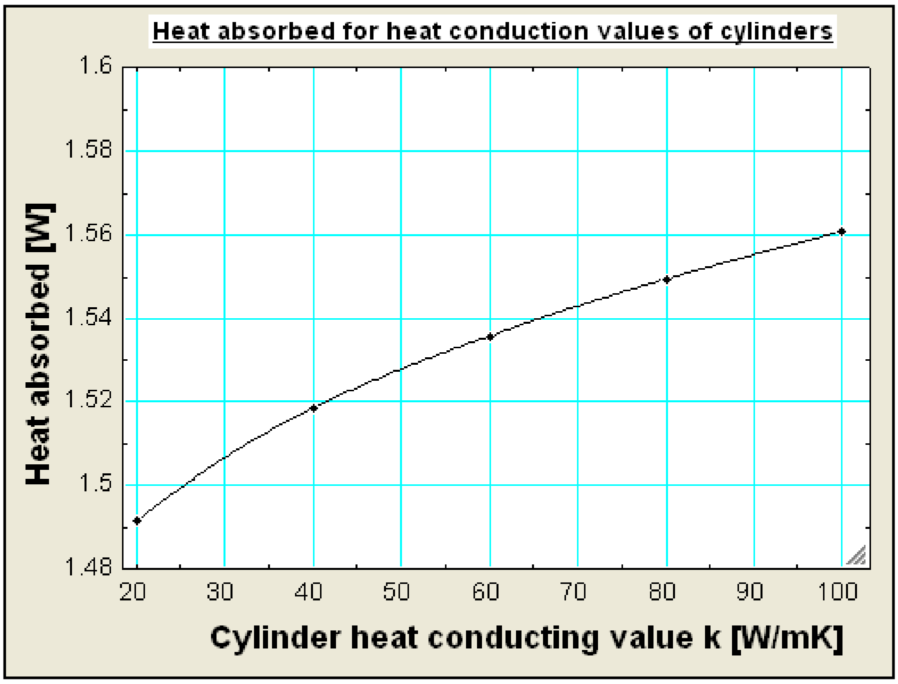

Figure 17: The relation between the amount of heat absorbed and the cylinder heat conducting value for increments between 20 W/mK and 100 W/mK.

Table 11: Energy absorbed for different heat conducting values of the cylinders between 5 W/mK and 20W/mK with 5 W/mK increments.

Cylinder thermal conductivity value [W/mK]	Energy absorbed [W]
5	1.44278
10	1.4675
15	1.48168
20	1.49194

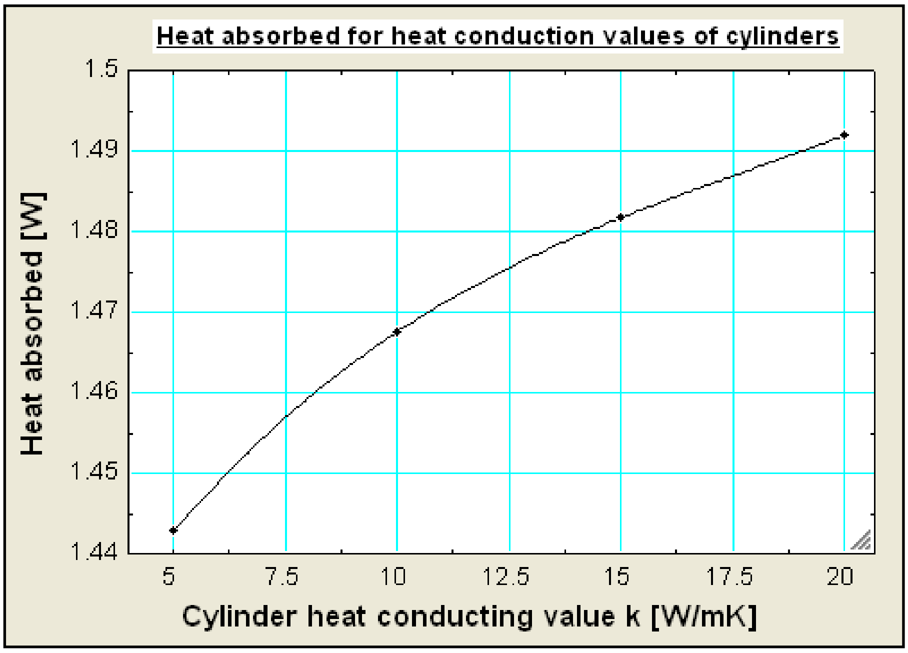

Figure 18: The relation between the amount of heat absorbed and the cylinder heat conducting value for increments between 5 W/mK and 20 W/mK.

6.4.2 Variation of thermal conductivity of the vacuum space

At first it could be argued that it is unnecessary to evaluate the thermal conductivity of the vacuum space. This is due to the expected logical implication (on heat transfer) of varying the thermal conductivity of a vacuum. However, although logical, these results remain very important for the purpose of comparison with other effects because of the numerical values associated with different scenarios. As mentioned earlier, this comparison and a discussion are done in the next chapter.

The variation of thermal conductivity of the vacuum implied that two sets of thermal conductivity values were selected and simulated for the vacuum. For the first set of simulations, the values varied from 0.001 W/mK to 0.01 W/mK with increments of 0.003 W/mK. The corresponding energy absorbed can be seen in Table 12 and Figure 19. For the second set increments of 0.0001 W/mK were used from 0.0001 W/mK to 0.0004 W/mK. From 0.0004 - 0.001 W/mK increments of 0.0003 W/mK were used. Parameters and results are given in Table 13 and Figure 20.

Table 12: Energy absorbed for thermal conductivity values of the vacuum between 0.001 and 0.01 W/mK.

Vacuum thermal conductivity value [W/mK]	Energy absorbed [W]
0.001	4.5732
0.004	16.15
0.007	27.716
0.01	39.268

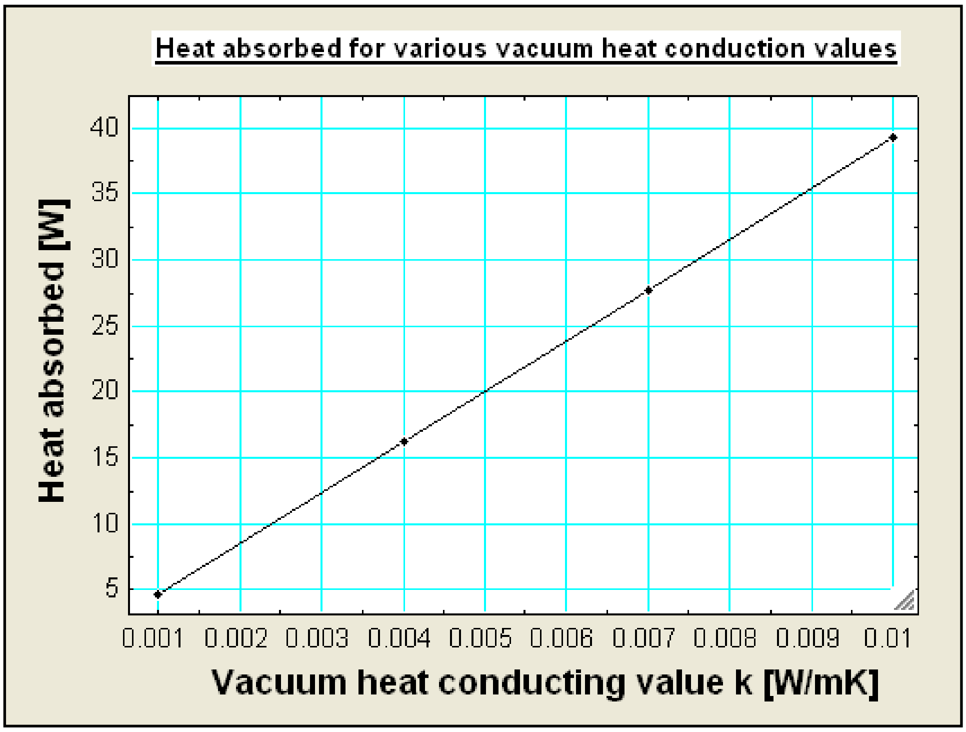

Figure 19: The relation between the amount of heat absorbed and the thermal conductivity of the vacuum for increments between 0.001 W/mK and 0.01 W/mK.

Table 13: Energy absorbed for thermal conductivity values of the vacuum between 0.0001 and 0.001 W/mK.

Vacuum thermal conductivity value [W/mK]	Energy absorbed [W]
0.0001	1.098
0.0002	1.484
0.0003	1.870
0.0004	2.256
0.0007	3.415
0.001	4.573

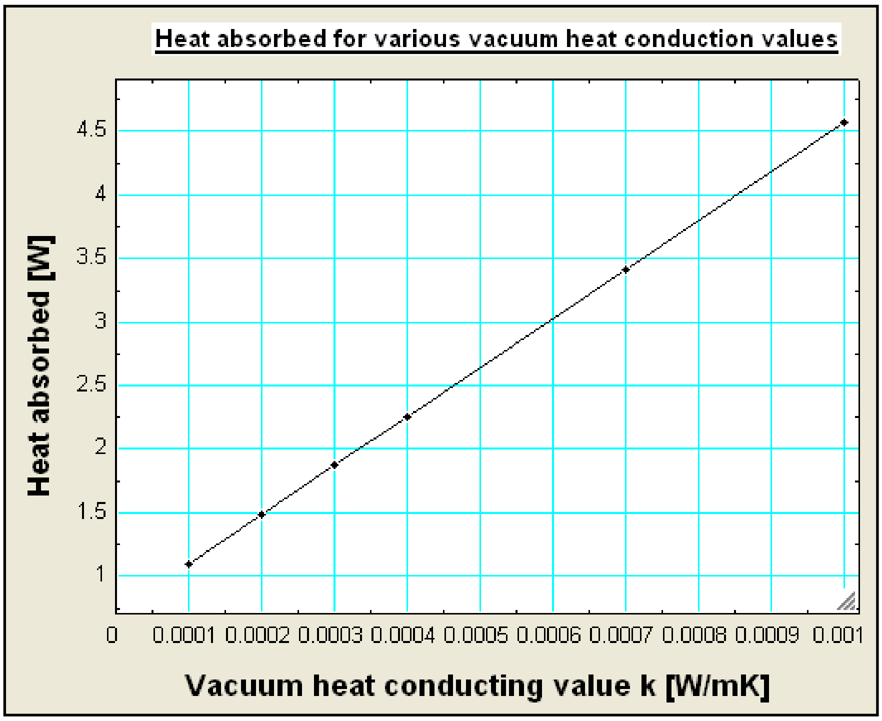

Figure 20: The relation between heat absorbed by the storage system and the heat conducting value of the vacuum for increments between 0.0001 W/mK and 0.001 W/mK.

6.4.3 Variation of ambient temperature

In this section the ambient temperature was varied to evaluate the effect thereof on the amount of heat absorbed by the system. For all other simulations the ambient temperature was set at 26°C. The effect is shown in Table 14 and Figure 21.

Table 14: The relation between the amount of heat absorbed and the ambient temperature.

Ambient temperature [°C]	Energy absorbed [W]
-50	1.0647
-25	1.20262
0	1.34052
25	1.47844
50	1.61636
75	1.75426

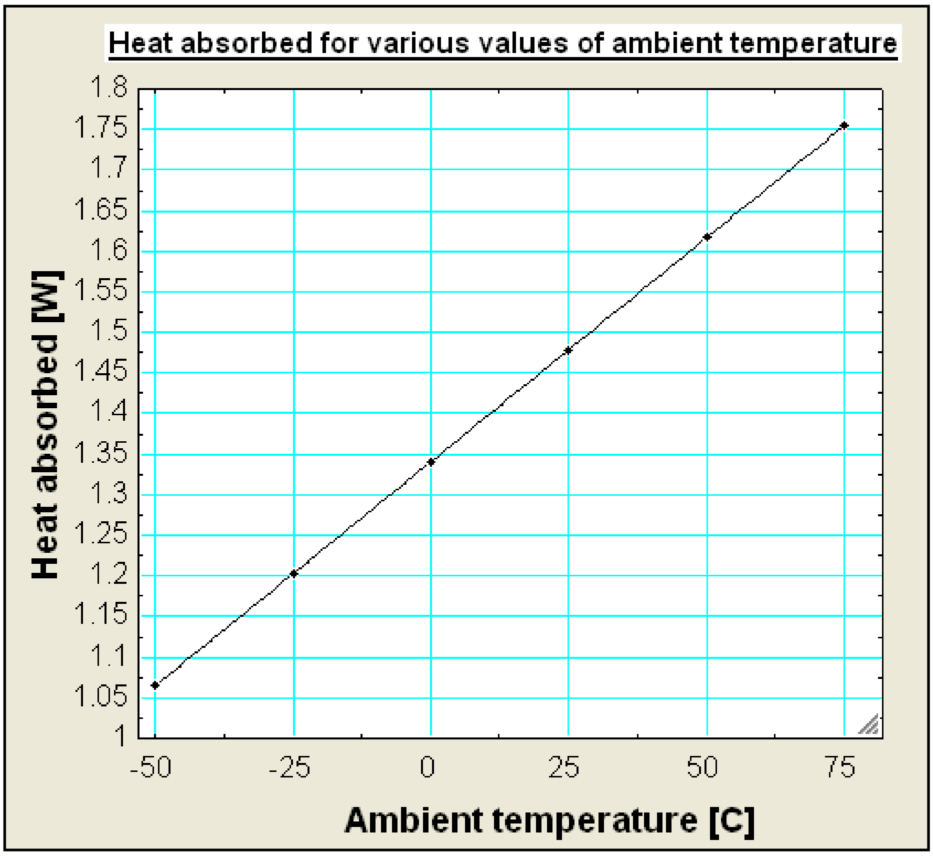

Figure 21: The relation between the amount of heat absorbed and the ambient temperature for temperatures ranging from -50°C to 75°C.

6.5 Verification of the FEA results

The final step of the thermal investigation was to verify whether the FEA results were realistic. This was done by comparing FEA results with results obtained from manual calculations.

If results in the same order are obtained both by manual calculation and by FEA simulation for more than one different set of conditions, it would point to high probability that both sets of results are realistic. If not, it would point out an error within either the manual calculations or the FEA simulations.

In order to verify the FEA results the following procedure was followed. A heat transfer model (with cylinder length of 800 mm and sphere radius of 150 mm) was solved both manually (as described earlier in paragraph 5.2) and by using FEA for thermal conductivity values from 0 W/mK to 0.002 W/mK. This thus yielded two sets of heat transfer results. A comparison of the two sets of results is given in Figure 22. The blue line represents the FEA results, while the results obtained from manual calculation (indicated in the figure as hand calculations) are represented by the black line.

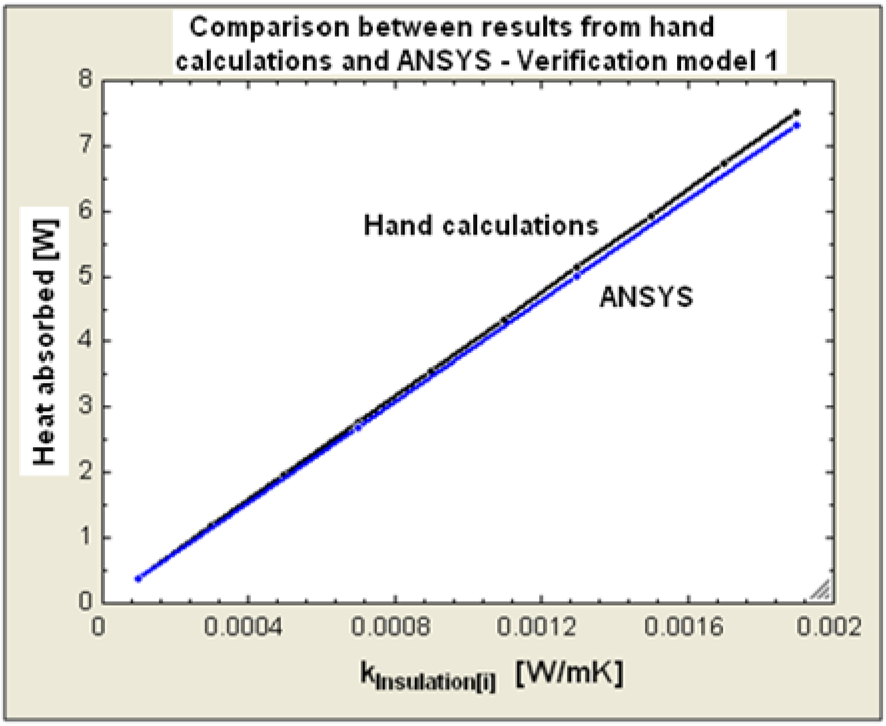

Figure 22: A comparison of results obtained from manual and FEA calculations showing the relation between the amount of heat absorbed and the thermal conductivity of the insulation for the given dimensions.

Results from this investigation show high accuracy for most thermal conductivities of the insulation. For heat conduction constants in the order lower than 0.0007 W/mK the results correspond almost exactly. At a thermal conductivity value of 0.002 W/mK, the correspondence is still above 95%.

Although very accurate, it is observed that the lines diverge slightly as thermal conductivity value increases. This observation can be explained by the fact that the model used in manual calculations and the model used for the FEA analysis did not correspond 100% geometrically. The model used for manual calculations did not include a hole where the nozzle fits, while the model used for FEA analysis did include a hole with a diameter of 10 mm. This meant that the total outer surface of the model used in manual calculations was 1.749 m^2, while the total outer surface of the FEA model was 0.000079 m^2 smaller. This explains why slightly higher heat absorption was evident for the model used in manual calculations.

However, although the two sets of results did not correspond exactly, the observed correspondence was still very high. Consequently it was concluded that the verification of the results points to a very high probability that the results from the ANSYS finite element analysis are realistic and accurate.

7. Discussion

As mentioned earlier, the previous chapter only included results. In this chapter the results and relevant observations are discussed. The following are notable observations worthy of discussion:

- The effect of a nozzle on boil-off.
- The effect of a nozzle on heat flux.
- The effect of a nozzle on the temperature profile in the system.
- The thermal conductivity of components.
- The effect of nozzle geometry.
- The effect of variations in ambient temperature.

7.1 The effect of a nozzle on boil-off

For the setup of constants and conditions as given in paragraph 5.4.2**,** the effect of the nozzle (with a thermal conductivity value of only 5 W/mK) used for hydrogen extraction, is that the amount of heat transfer into the inner cylinder almost doubles. This means that the amount of boil-off also doubles, pointing to a massive loss of energy in the form of hydrogen due to the presence of a nozzle extraction system. For a nozzle with thermal conductivity of 20 W/mK the effect is that the daily amount of hydrogen lost due to boil-off is predicted to be 0.21 kg. This is equivalent to about 15.6 liters of gasoline.

Considering a vehicle with low fuel consumption of 25 km per liter gasoline, the effect of such a nozzle extraction system is that a vehicle will potentially lose out on about 390 kilometers daily due to boil-off caused by the presence of a nozzle.

Even for a nozzle with thermal conductivity of only 5 W/mK, the equivalent travel distance lost is still 145 km.

This indicates that a permanent nozzle extraction system will only be viable if the thermal conductivity value of the nozzle is below 2.5 W/mK. This takes into consideration that the average vehicle travels about 70 km daily.

7.2 The effect of a nozzle on heat flux

As expected, results showed that the base model had a much lower maximum heat flux than the model with the nozzle. For the base model the maximum heat flux occurred at the spherical ends of the system. This phenomenon can be explained by the fact that the ratio of inner to outer area is smaller for a thick wall sphere than for a thick wall cylinder with the same radius. This indicates that the nozzle position also plays a part in boil-off.

As expected for the model with the nozzle, the maximum heat flux occurred in the nozzle region, as shown below in Figure 23. Although heat flux through the rest of the storage system still exists, it becomes almost negligibly small.

For the model with the nozzle the heat flux into the inner cylinder is the main contributor to boil-off. Because of the magnitude of the heat flux observed in the simulation, it is logically expected that it would cause a drastic rise in boil-off. This observation supports the results of the massive increase in boil-off due to the nozzle system.

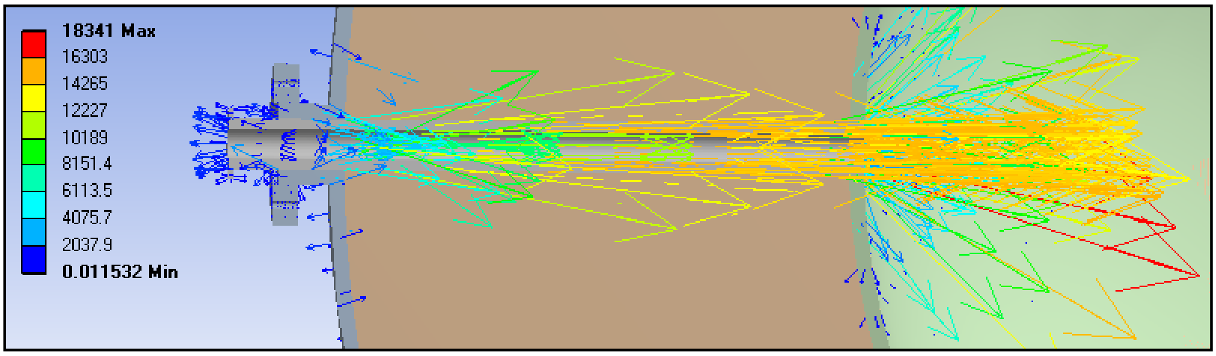

Figure 23: Vectors representing the magnitude of heat flux [W/m^2] through the nozzle area of the storage system.

The heat flux phenomenon illustrated here clearly indicates the effect of the nozzle on the system. Keeping in mind that the secondary aim of the system is to minimize boil-off, the image and values above clearly indicate a thermal breach being created by the nozzle extraction system, having drastic effects on boil-off.

7.3 The effect of a nozzle on the temperature profile

From the obtained results it is concluded that the effect of the nozzle extraction system on the temperature and the temperature profile is very small. The only change observed is a small increase in the maximum temperature of the outer surface of the system. On inspection of the temperature profile shown in Figure 24, it is strangely observed that the temperature profile is shaped outwards towards the feed tube and bracket and not inwards as first instincts would expect.

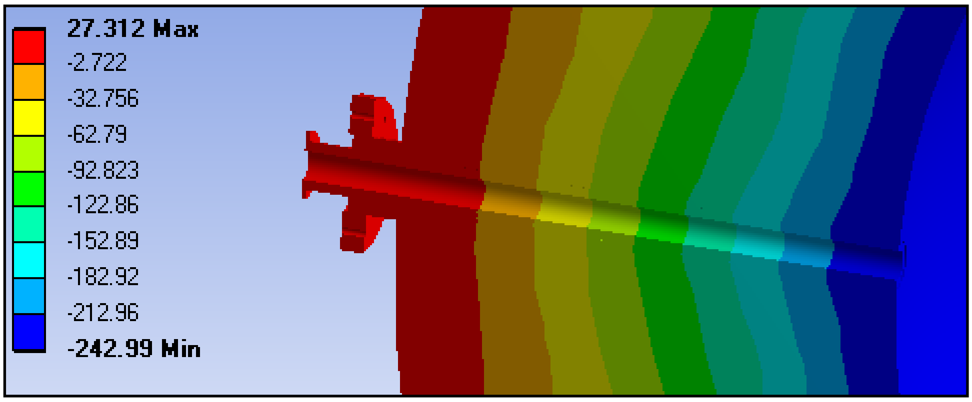

Figure 24: A graphical representation of the indentation of the temperature profile [°C] in the vicinity of the nozzle.

However, the temperature profile is explainable. It is known from heat transfer principles that the inner cylinder should warm up as the nozzle conducts heat into it. However, as observed here, this is not the case. The reason is that the inner cylinder temperature is fixed for the simulation. The reason for using a fixed temperature on the inner cylinder is that, in the process of boiling, the available energy is absorbed by the hydrogen in the process of the phase change from liquid to gas. Only once all the hydrogen is in gaseous state will the temperature start to rise.

This explains why the temperature profile is shaped outwards and why the minimum temperature did not rise as expected.

It should also be considered that the nozzle immediately cools down because of the contact with the very low temperature of the wall of the inner cylinder. The cooled down nozzle then cools down the area around its contact point with the inner cylinder, also explaining the temperature profile observed.

7.4 The thermal conductivity of components

The variation of thermal conductivity values of the component materials had a direct and considerable impact on heat transfer and the resulting boil-off. The most sensitive component is undoubtedly the vacuum space used for insulation. In terms of associated heat transfer and boil-off, the vacuum is about 500 times more sensitive to changes in the thermal conductivity value than the cylinder material. This clearly indicates that the vacuum is effectively the sole insulating component. A very slight change in the thermal conductivity value of the vacuum caused massive changes in boil-off.

The second most sensitive component is the nozzle. In terms of associated heat transfer, the nozzle material is about 13.5 times less sensitive to changes in thermal conductivity value than the vacuum. Although considerably less sensitive than the vacuum, its effect is still of a magnitude that has the potential to drastically influence the system's viability. This is due to the fact that the thermal conductivity value used for the nozzle is generally much higher than that of the vacuum (for this study the difference was just below 5 W/mK). This explains why, even though the vacuum space is more sensitive, the addition of the nozzle caused such a massive increase in boil-off.

It should also be kept in mind that although not the most sensitive to change in thermal conductivity, the nozzle is still the main contributor towards heat flow into the system. On this basis, the nozzle is considered to be the main drawback of this system due to the associated boil-off it causes.

The inner and outer cylinder material is evidently the least sensitive to changes in thermal conductivity. Changes in the thermal conductivity of the cylinders had about 37 times less influence on boil-off than the nozzle material. This may be explained by the fact that the vacuum is such an effective insulator, that it allows almost no heat into the system to be conducted by the cylinder walls. This means that in the selection of material for the inner and outer cylinder, that the thermal conductivity of the material is not limited to extremely low values. However, this is only true if the vacuum insulation is of outstanding quality.

From the results it is observed that the heat absorption and corresponding boil-off increase linearly as the thermal conductivity of the nozzle material and vacuum space increases. For the inner and outer cylinder material this increase is not linear, but it declines for higher thermal conductivity values. This can be explained by the fact that, for a higher thermal conductivity, the cylinders extract and conduct more heat from the nozzle than for a lower cylinder thermal conductivity. Although the higher thermal conductivity value allows a larger overall heat flow into the system, the amount of heat flow from the nozzle to the cylinders and from the outer cylinder to the environment also increases, thus having the effect of a decline in the gradient of the graph. This explanation is supported by Figure 23, where it is observed that vectors representing heat flux, point outwards into the environment, meaning that to some degree heat is conducted from the nozzle to the environment via the outer cylinder.

7.5 The effect of nozzle geometry

The effect of varying the nozzle geometry and cross sectional area has significant impact on heat transfer and boil-off. For a reduction of wall thickness from 2 mm to 0.5 mm, a 33.3% reduction in heat transfer was achieved, indicating the importance of minimizing this area.

It was also observed that the heat flow into the inner cylinder is not a linear function of the total nozzle cross-sectional area. For a smaller total cross-sectional nozzle area, the corresponding amount of heat flow is, as expected, lower than for a nozzle with a larger total cross-sectional nozzle area; however the rate of reduction of heat transfer does not correspond with the rate of nozzle area reduction.

This phenomenon can be explained by the fact that a linear reduction of the nozzle wall thickness causes a non-linear decrease in the nozzle cross-sectional area. This non-linear nozzle cross-sectional area reduction explains the non-linear reduction in the amount of energy transferred into the system.

7.6 The effect of ambient temperature

In terms of the effect of ambient temperature surrounding the outer cylinder, alterations thereof showed only a small difference in the amount of heat absorbed. For every 10°C increase in ambient temperature, the amount of energy absorbed only increased by about 0.056 Watt. This indicates that the effect of ambient temperature is very small in comparison with the thermal conductivity of both the nozzle and the vacuum. This is due to the very low thermal conductivity of the vacuum, minimizing the effect of external thermal impacts on the liquid hydrogen.

8. Conclusion

From the results and discussion, the following conclusions are made:

- Although the use of cryogenic hydrogen storage shows promising potential in terms of both volumetric and gravimetric capacities, it is not yet at a level where it can be efficiently implemented for vehicular application.
- It is also concluded that the general trend of cryogenic hydrogen storage systems is that hydrogen will be lost in an environment at normal conditions as time goes by. This indicates that the application of cryogenic hydrogen storage systems is limited.
- It is concluded that any nozzle extraction system (even with low nozzle thermal conductivity values) will cause a considerable increase in hydrogen boil-off. Even for sophisticated technology, the boil-off of hydrogen increases considerably when the nozzle is used for extraction purposes. The main issue is that the nozzle system creates a thermal breach leading to a large increase in heat transfer, accompanied by an increase in hydrogen boil-off. The increase in boil-off due to the use of a nozzle with thermal conductivity above 2.5 W/mK is of such magnitude that the cryogenic storage will not be viable for vehicular use.
- In terms of the nozzle, it is concluded that the effect nozzle geometry alteration has significantly less influence on boil-off than the nozzle material thermal conductivity. The nozzle system does not affect the temperature distribution in the system to such an extent that it causes concern, however the heat flux through the nozzle is an issue of greater consequence. The difference in maximum heat flux between the nozzle and a no-nozzle system is astronomical, once again indicating the issue of heat conduction by the extraction system.
- Evaluation of the thermal conductivity of the cylinders and vacuum showed that alteration of the thermal conductivity of the vacuum had a much more profound effect than that of alteration of thermal conductivity values of the cylinders.

Variation of ambient temperatures showed a very small effect in terms of changes in the amount of boil-off.

- In terms of the geometry of heat transfer, it was shown that the heat flux in the system is concentrated at the two spherical ends of the storage system. This means that the position of the nozzle extraction system may have an effect on overall boil-off.
- Depending on the application of the vehicle, boil-off may be considered as an advantage, since it may function as an automatic fuel delivery system. However, the downside to this is that the vehicle application will have to be specific and constant; otherwise it may result in blow-off or even a stranded driver.
- It should also be considered that, if the vehicle is used regularly, an acceptable level of boil-off exists. What this means is that, if the vehicle consumes more (or the same amount) of hydrogen than what boils off, it would effectively mean that the vehicle does not lose out on any energy, although the storage system itself may experience boil-off. It is thus concluded that the viability of the system is largely dependent on the specific application of the vehicle.
- In terms of safety, the system shows no considerable concern. The biggest possible issue may be self-pressurization due to boil-off, but it can be managed by means of blow-off. Another safety issue that may arise in the case of an accident is liquid hydrogen spillage.

9. Recommendations

It is firstly recommended that another type of extraction system should be evaluated where (if possible) no nozzle is used. This will eliminate the thermal breach created by the nozzle. It will also compliment the sophisticated isolation system, rather than compromising its isolation capability.

However, if a nozzle has to be used, a transient extraction system is recommended. The nozzle system is then only used in cases either when self-pressurization due to boil-off creates an unsafe gas pressure, or when the vehicle demands fuel for propulsion. What this means is that the advantages of a no-nozzle system can be combined with a nozzle extraction system, possibly leading to lower overall boil-off. However, it should be considered that this system will be more complex.

The third recommendation is that a secondary system should be in place to absorb the heat transferred through the nozzle. This means that the liquid hydrogen will not experience the effect of the heat flow, since it will be absorbed by the secondary system. Currently, a very promising secondary system is one that uses the boil-off of liquid nitrogen as a barrier to isolate the liquid hydrogen (Van Vuuren *et al.*, 2009).

It is also recommended that the nozzle itself be optimized in terms of isolation, material, geometry and thermal conductivity with the aim of lowering levels of boil-off. However, a very sophisticated nozzle (associated with high cost) will be required due to the extreme temperature gradient experienced in cryogenic applications.

Another recommendation is to pre-cool the nozzle before the process of hydrogen extraction starts. This could possibly level out the massive temperature gradient experienced at the contact surface between the nozzle and inner cylinder. However, it should be kept in mind that the process of cooling the nozzle will in itself consume energy, possibly be complex and costly. An energy analysis comparing the energy required for cooling versus the amount of energy conserved due to a decrease in boil-off will be required to determine the viability this recommendation.

Finally, since the geometry of heat transfer showed that the heat flux is more concentrated in certain areas of the system, it is recommended that the effect of the nozzle position should be investigated. This confirms the findings of Ho and Rahman (2007) who concluded that the temperature profile of the system is indirectly linked to nozzle position.

Bibliography

Aceves, S.M., Espinosa-Loza, F., Ledesma-Orozco, E., Ross, T.O., Weisberg, A.H., Brunner, T.C. & Kircher, O. 2009. High-density automotive hydrogen storage with cryogenic capable pressure vessel. *International Journal of hydrogen energy*, 35:1219-1226.

Aceves, S.M., Martinez-Frias, J. & Garcia-Villazana, O. 2000. Analytical and experimental evaluation of insulated pressure vessels for cryogenic hydrogen storage. *International journal of hydrogen energy,* 25:1075-1085.

Ahluwalia, R.K. & Peng, J.K. 2008. Dynamics of cryogenic hydrogen storage in insulated pressure vessels for automotive applications. *International journal of hydrogen energy*, 33: 4622-4633. May.

Ahluwalia, R.K., Hua, T.Q. & Peng, J.K. 2011. On-board and off-board performance of hydrogen storage options for light-duty vehicles. *International journal of hydrogen energy*, June.

Alonso, J.C.Q. Alonso formula. 2010. http://www.alonsoformula.com/inorganic/hidruros.htm Date of access: 19 Apr. 2010.

Anon. s.a. IEA world energy outlook 2008 reference case. http://www.iosa.ca/the_issues/energy_supply/ Date of access: November 2011.

Anon. s.a. Metal hydride hydrogen storage. http://www.hydrogengas.biz/images/page13image.jpg Date of access: December 2011.

Barcelo, S., Rogers, M., Grigoropoulos, C. & Mao, S. 2010. Hydrogen storage property of sandwiched magnesium hydride nanoparticle thin film. *International journal of hydrogen energy*, 1-4. January.

Bossel, U. & Eliasson, B. 2003. Energy and the hydrogen economy. *Hydrogen economy report 2003.* http://www.methanol.org/pdf/HydrogenEconomyReport 2003.pdf.

Champagne, V.K., Leyman, P.F. & Helfritch, D.J. 2008. Magnesium repair by cold spray. *Weapons and materials research directorate*, May.

Collins English Dictionary. 2009. 10th Ed. William Collins Sons & Co. Ltd.

De Oliveira Matias, J.C. & Devezasa, T.C. 2007. Consumption dynamics of primary-energy sources: the century of alternative energies. *Applied energy* 84(7-8):763-770.

Dillich, S. 2009. Hydrogen storage program element introduction. US Department of Energy. http://www.hydrogen.energy.gov/pdfs/progress09/iv_0_hydrogen_storage_overview.pdf Date of acces 21 Apr. 2010).

Heung, L.K. 2003. Using metal hydride to store hydrogen. Fuel Cells 2003 -Third Annual BCC Conference, Stamford.

Ho, S.H. & Rahman, M.M. 2007a. Nozzle injection displacement mixing in a zero boil-off hydrogen storage tank. *International journal of hydrogen energy,* 33:878-888.

Ho, S.H. & Rahman, M.M. 2007b. Three-dimensional analysis for liquid hydrogen in a cryogenic storage tank with heat pipe system. *Cryogenics,* 48:31-41.

Incropera, F.P., DeWitt, D.P., Bergman, T.L. & Lavine, A.S. 2007. Fundamentals of heat and mass transfer. 6th Ed. Indiana: John Wiley.

Jain, I.P., Chhagan L. & Ankur, J. 2009. Hydrogen storage in Mg: a most promising material. *International journal of hydrogen energy,* 1-12. August.

Jianglan, Q., Sun, B., Rong, Y., Zhao, W., Wang, Y. & Li, X. 2009. Hydrogen absorption kinetics of Mg thin films under mild conditions. *Scripta materialia,* 62: 317-320. November.

Johnston, B., Mayo, M.C. & Khare, A. 2005. Hydrogen: the energy source for the 21st century. *Tecnovation,* 25(6). June.

Jorgensen, S.W. 2010. Hydrogen storage tanks for vehicles: recent progress and current status. *Current opinion in solid state and materials science,* 15:39-43.

Kumar, V.S. & Kumar, S. 2010. Generalized model development for a cryo-adsorber and 1-D results for the isobaric refueling period. *International journal of hydrogen energy*, 35: 3598-3609.

Li, Z., Xu, L., Sun, H., Xiao, Y. & Zhang, J. 2004. Investigation on performances of non-loss storage for cryogenic liquefied gas. *Cryogenics*, 44:357-362.

Magnesium.com. 2011. Magnesium encyclopedia properties. http://www.magnesium.com/w3/data-bank/index.php?mgw=153.

MAN Diesel. 2010. Influence of Ambient Temperature Conditions on Main Engine Operation of MAN B&W Two-stroke Engines. 2010. http://www.mandiesel.com/files/news/filesof762/5510-0005.pdf.

Pourpoint, T.L., Velagapudi, V., Mudawar, I., Zheng, Y. & Fisher, T.S. 2010. Active cooling of a metal hydride system for hydrogen storage. *International journal of heat and mass transfer*, 53(7-8):1326-1332.

Pranevicius, L., Milcius, D., Templier, C., Pranevicius, L.L. & Lelis, M. 2009. Studies of Mg film and substrate coupling effects on hydrogenation properties. *Journal of alloys and compounds*, 488:360–363. August.

Salameh, M.G. 2002. Can renewable and unconventional energy sources bridge the global energy gap in the 21st century? *Applied energy* 75:33-42. November.

Sarkar A. & Banerjee R. 2004. Net energy analysis of hydrogen storage options. *International journal of hydrogen energy* 30(8):867-877.

Satyapal, S., Petrovic, J., Read, C., Thomas, G. & Ordaz, G. 2007. The U.S. Department of Energy's national hydrogen storage project: progress towards meeting hydrogen-powered vehicle requirements. *Catalysis today*, 120: 246-256.

Seo, M. & Jeong, S. 2010. Analysis of self-pressurization phenomenon of cryogenic fluid storage tank with thermal diffusion model. *Cryogenics*, 50:549-555.

Tan, X., Harrower, C.T., Harrower, B.S. & Mitlin, D. 2009. Nano-scale bi-layer Pd/Ta, Pd/Nb, Pd/Ti and Pd/Fe catalysts for hydrogen sorption in magnesium thin films ." *International journal of hydrogen energy* , 34(18):7741-7748 .

The American Heritage® Dictionary of the English Language. 2000. 4th Ed. Houghton Mifflin Company.

UIC (Universal Industrial Gases Inc.). 2007. Hydrogen (H_2) properties, uses, applications: hydrogen gas and liquid hydrogen. http:/www.uigi.com/hydrogen.

Van Antwerpen, W. 2009. Modelling the effective thermal conductivity in the near-wall region of a packed pebble bed. Potchefstroom: NWU. (Thesis - PhD).

Van den Biggelaar, M. 2010. The key to making lightweight cars. Schwalbach: Dow Automotive Systems.

Van Vuuren, D.S., Hietkamp, S. & Benson, J. 2009. Cryogenic compressed hydrogen storage. South African Chemical Engineering Congress, Somerset West.

Von Kaufmann, K.H. 2004. The solar economy: renewable energy for a sustainable future. *Futures,* 36(10). December.

Willisms.com. s.a. World energy demand. http://www.willisms.com/archives/asianoil demand.gif Date of access: December 2011.

Zhou, L. 2005. Progress and problems in hydrogen storage methods. *Renewable and sustainable energy reviews*, 9(4): 395-408.

Appendix A: Storage system drawings

Storage system

The components of the cryogenic hydrogen storage system as created virtually in SolidWorks® are shown in Appendix A. Since the system is virtual, no tolerances are included.

Detail drawings of the following components are included:

1. Inner cylinder
2. Vacuum space
3. Outer cylinder
4. Nozzle 1
5. Nozzle 2
6. Nozzle 3
7. Nozzle 4

Inner cylinder

Vacuum space

Outer cylinder

Nozzle 1

Nozzle 2

Nozzle 3

Nozzle 4

Appendix B: Simulation Procedure

ANSYS simulation procedure and project report

In this appendix a summarized simulation procedure is given, followed by an example of a partial ANSYS project report. Only the most important sections of the project report are given in this appendix. The full ANSYS Project report is available on the electronic attachment. All the simulations were done based on the same generic procedure and parameters as presented in this appendix.

The simulation and corresponding procedure can be divided into three branches namely Modal, Steady-state Thermal and a Solution Branch.

In the modal branch the geometry, coordinate system, connections and mesh inputs are made. In the geometry branch materials are assigned to the individual parts. The following were settings made for all parts in terms of geometry:

- The selected stiffness behavior is set to be flexible.
- The reference temperature is the environment temperature.
- In terms of materials both nonlinear effects and thermal strain effects are taken into consideration.
- The volume, mass and moment of inertia of all the individual parts were also checked in the modal branch.

Under the modal branch connections settings for all contact areas were made. Firstly the contact areas were checked to ensure that the right amount of contact areas existed. The following settings were made for all contact areas:

- All contact surfaces were assumed to be bonded together for the entire simulation.
- The behavior of all contact surfaces was symmetric.
- The thermal conductance of contact surfaces were program controlled.
- ANSYS uses a “pinball” to evaluate whether two surfaces are in contact or not. Altering the size of the pinball can thus determine whether two regions will be considered to be in contact or not. When needed the pinball radius was altered to open and close contact surfaces for purposes of simulation.

In the steady state branch all the thermal entities needed for the simulation were entered. These included ambient and surface temperatures, convection constants, conduction constants, fluid temperatures as well as areas of perfect insulation. These entities were set according to the effect that is being investigated.

The following settings were also made in this branch:

- The initial temperature was set.
- The analysis settings were made.
- Convection conditions and constants were entered for all components occupying space.

In the solution branch solution information may be acquired in two ways. Firstly, by means of the solution information solver output document. This document is generated and contains all simulation data and is shown in the next section. The second is by inserting a thermal temperature, heat flux and directional heat flux in the solution branch. Examples of solver output for temperature and heat flux are given by Figure 25 and Figure 26 respectively.

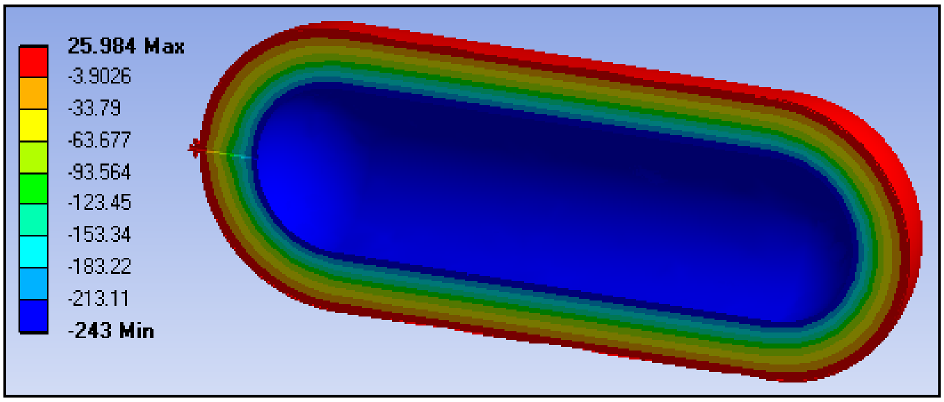

Figure 25: Solution branch: Thermal temperature

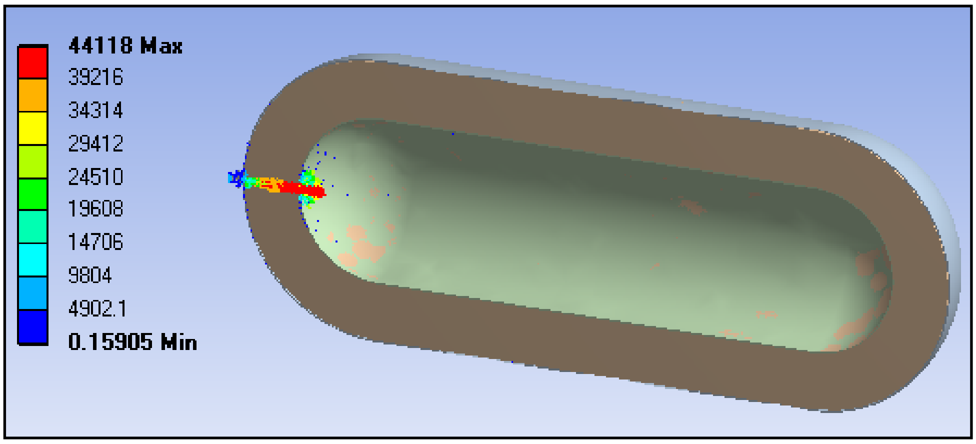

Figure 26: Solution branch: Thermal heat flux

To take virtual measurements of a certain data or information in ANSYS, for example to measure the heat flux over a certain area, a reaction probe is used. This is a tool built into the ANSYS results branch to give the user the ability to extract results in a simple manner.

Where it was required, a reaction probe was inserted to measure the total amount of heat flow and heat flux.

Project

First Saved	Thursday, September 08, 2011
Last Saved	Monday, September 26, 2011
Product Version	13.0 Release

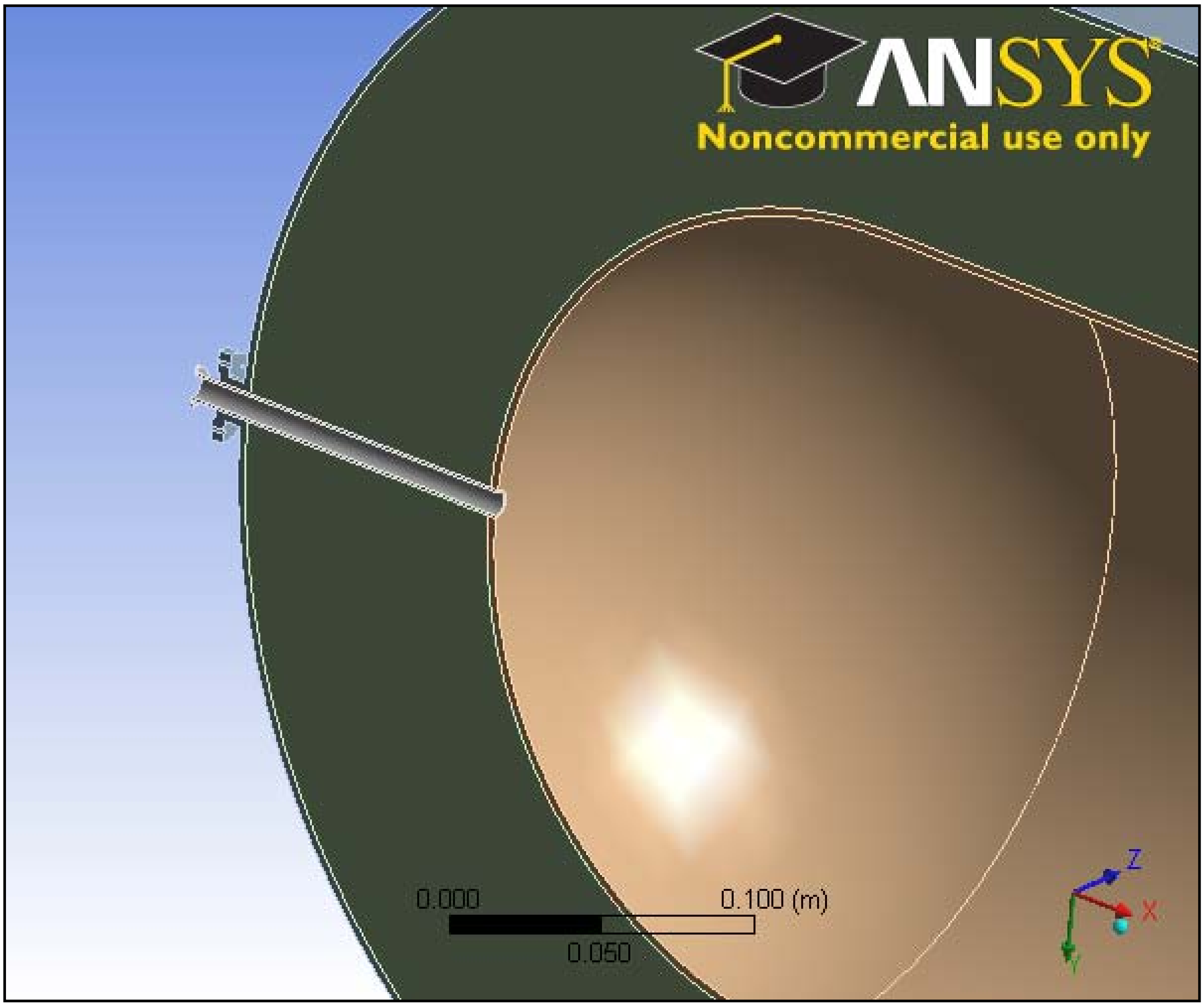

Contents

Units

TABLE 1

Unit System	Metric (m, kg, N, s, V, A) Degrees RPM Celsius
Angle	Degrees
Rotational Velocity	RPM
Temperature	Celsius

Model (A4)

Geometry

TABLE 2
Model (A4) > Geometry

Object Name	*Geometry*
State	Fully Defined
Definition	
Source	C:\Documents and Settings\Administrator\Desktop\Solidworks\TOETSE\Models for evaluation of nozzle geometry\Nozzle geometry 3\Nozzle 3.SLDASM
Type	SolidWorks
Length Unit	Meters
Element Control	Program Controlled
Display Style	Part Color
Bounding Box	
Length X	1.3219 m
Length Y	0.502 m

Length Z	0.25058 m
Properties	
Volume	7.9483e-002 m^3
Mass	35.84 kg
Scale Factor Value	1.
Statistics	
Bodies	4
Active Bodies	4
Nodes	24689
Elements	12921
Mesh Metric	None
Preferences	
Import Solid Bodies	Yes
Import Surface Bodies	Yes
Import Line Bodies	No
Parameter Processing	Yes
Personal Parameter Key	DS
CAD Attribute Transfer	No
Named Selection Processing	No
Material Properties Transfer	No
CAD Associativity	Yes
Import Coordinate Systems	No
Reader Save Part File	No
Import Using Instances	Yes
Do Smart Update	No
Attach File Via Temp File	Yes
Temporary Directory	C:\Documents and Settings\Administrator\Local Settings\Temp
Analysis Type	3-D
Mixed Import Resolution	None
Enclosure and Symmetry Processing	Yes

TABLE 3
Model (A4) > Geometry > Parts

Object Name	*Extraction nozzle 3-1*	*Outer cylinder no extraction nozzle 3 (2)-1*	*Vacuum no extraction nozzle 3-1*	*Inner cylinder no extraction nozzle 3 (1)-1*
State	Meshed			
Graphics Properties				
Visible	Yes			
Transparency	1			
Definition				
Suppressed	No			
Stiffness Behavior	Flexible			
Coordinate System	Default Coordinate System			
Reference Temperature	By Environment			
Material				
Assignment	Nozzle material	Structural Steel	Vacuum	Structural Steel
Nonlinear Effects	Yes			
Thermal Strain Effects	Yes			
Bounding Box				
Length X	0.126 m	1.313 m	1.2959 m	1.0959 m
Length Y	1.4e-002 m	0.502 m	0.496 m	0.296 m
Length Z	7.e-003 m	0.25058 m	0.24758 m	0.14765 m
Properties				
Volume	1.819e-006 m³	3.0566e-003 m³	7.4915e-002 m³	1.509e-003 m³
Mass	0. kg	23.994 kg	0. kg	11.846 kg
Centroid X	-0.70921 m	-0.10059 m	-0.1 m	-0.10077 m
Centroid Y	-2.0319e-017 m	1.0206e-005 m	5.7677e-007 m	9.5416e-006 m
Centroid Z	2.8803e-003 m	0.14547 m	0.11996 m	8.7741e-002 m
Moment of Inertia Ip1	0. kg·m²	0.78766 kg·m²	0. kg·m²	0.13912 kg·m²
Moment of Inertia Ip2	0. kg·m²	4.0089 kg·m²	0. kg·m²	1.2005 kg·m²
Moment of Inertia Ip3	0. kg·m²	3.503 kg·m²	0. kg·m²	1.2914 kg·m²
Statistics				
Nodes	798	9354	9655	4882
Elements	90	4589	5882	2360
Mesh Metric	None			

Coordinate Systems

TABLE 4
Model (A4) > Coordinate Systems > Coordinate System

Object Name	*Global Coordinate System*
State	Fully Defined
Definition	
Type	Cartesian
Coordinate System ID	0.
Origin	
Origin X	0. m
Origin Y	0. m
Origin Z	0. m
Directional Vectors	
X Axis Data	[1. 0. 0.]
Y Axis Data	[0. 1. 0.]
Z Axis Data	[0. 0. 1.]

Connections

TABLE 5
Model (A4) > Connections

Object Name	*Connections*
State	Fully Defined
Auto Detection	
Generate Automatic Connection On Refresh	Yes
Transparency	
Enabled	Yes

TABLE 6
Model (A4) > Connections > Contacts

Object Name	*Contacts*
State	Fully Defined
Definition	
Connection Type	Contact
Scope	
Scoping Method	Geometry Selection
Geometry	All Bodies
Auto Detection	
Tolerance Type	Slider
Tolerance Slider	0.
Tolerance Value	3.5901e-003 m
Face/Face	Yes
Face/Edge	No
Edge/Edge	No
Priority	Include All
Group By	Bodies
Search Across	Bodies

TABLE 7
Model (A4) > Connections > Contacts > Contact Regions

<table>
<tr><td>Object Name</td><td>Contact Region</td><td>Contact Region 2</td><td>Contact Region 3</td><td>Contact Region 4</td><td>Contact Region 5</td></tr>
<tr><td>State</td><td colspan="5">Fully Defined</td></tr>
<tr><td colspan="6">Scope</td></tr>
<tr><td>Scoping Method</td><td colspan="5">Geometry Selection</td></tr>
<tr><td>Contact</td><td colspan="3">1 Face</td><td colspan="2">3 Faces</td></tr>
<tr><td>Target</td><td>2 Faces</td><td colspan="2">1 Face</td><td colspan="2">3 Faces</td></tr>
<tr><td>Contact Bodies</td><td colspan="3">Extraction nozzle 3-1</td><td>Outer cylinder no extraction nozzle 3 (2)-1</td><td>Vacuum no extraction nozzle 3-1</td></tr>
<tr><td>Target Bodies</td><td>Outer cylinder no extraction nozzle 3 (2)-1</td><td>Vacuum no extraction nozzle 3-1</td><td>Inner cylinder no extraction nozzle 3 (1)-1</td><td>Vacuum no extraction nozzle 3-1</td><td>Inner cylinder no extraction nozzle 3 (1)-1</td></tr>
<tr><td colspan="6">Definition</td></tr>
<tr><td>Type</td><td colspan="5">Bonded</td></tr>
<tr><td>Scope Mode</td><td colspan="5">Automatic</td></tr>
<tr><td>Behavior</td><td colspan="5">Symmetric</td></tr>
<tr><td>Suppressed</td><td colspan="5">No</td></tr>
<tr><td colspan="6">Advanced</td></tr>
<tr><td>Formulation</td><td colspan="5">Pure Penalty</td></tr>
<tr><td>Thermal Conductance</td><td colspan="5">Program Controlled</td></tr>
<tr><td>Pinball Region</td><td colspan="5">Program Controlled</td></tr>
</table>

Mesh

TABLE 8
Model (A4) > Mesh

Object Name	*Mesh*
State	Solved
Defaults	
Physics Preference	Mechanical
Relevance	0
Sizing	
Use Advanced Size Function	Off
Relevance Center	Coarse
Element Size	1.e-002 m
Initial Size Seed	Active Assembly
Smoothing	Medium
Transition	Fast
Span Angle Center	Coarse
Minimum Edge Length	1.e-003 m
Inflation	
Use Automatic Inflation	None
Inflation Option	Smooth Transition
Transition Ratio	0.272
Maximum Layers	5
Growth Rate	1.2
Inflation Algorithm	Pre
View Advanced Options	No
Advanced	
Shape Checking	Standard Mechanical

Element Midside Nodes	Program Controlled
Straight Sided Elements	No
Number of Retries	Default (4)
Extra Retries For Assembly	Yes
Rigid Body Behavior	Dimensionally Reduced
Mesh Morphing	Disabled
Defeaturing	
Pinch Tolerance	Please Define
Generate Pinch on Refresh	No
Automatic Mesh Based Defeaturing	On
Defeaturing Tolerance	Default
Statistics	
Nodes	24689
Elements	12921
Mesh Metric	None

TABLE 9
Model (A4) > Mesh > Mesh Controls

Object Name	*Body Sizing*
State	Fully Defined
Scope	
Scoping Method	Geometry Selection
Geometry	3 Bodies
Definition	
Suppressed	No
Type	Element Size
Element Size	5.e-002 m
Behavior	Soft

Steady-State Thermal (A5)

TABLE 10
Model (A4) > Analysis

Object Name	*Steady-State Thermal (A5)*
State	Solved
Definition	
Physics Type	Thermal
Analysis Type	Steady-State
Solver Target	Mechanical APDL
Options	
Generate Input Only	No

TABLE 11
Model (A4) > Steady-State Thermal (A5) > Initial Condition

Object Name	*Initial Temperature*
State	Fully Defined
Definition	
Initial Temperature	Uniform Temperature
Initial Temperature Value	26. °C

TABLE 12
Model (A4) > Steady-State Thermal (A5) > Analysis Settings

Object Name	*Analysis Settings*
State	Fully Defined
Step Controls	
Number Of Steps	1.
Current Step Number	1.
Step End Time	1. s
Auto Time Stepping	Program Controlled
Solver Controls	
Solver Type	Program Controlled
Radiosity Controls	
Flux Convergence	1.e-004
Maximum Iteration	1000.
Solver Tolerance	0.1
Over Relaxation	0.1
Hemicube Resolution	10.
Nonlinear Controls	
Heat Convergence	Program Controlled
Temperature Convergence	Program Controlled
Line Search	Program Controlled
Output Controls	
Calculate Thermal Flux	Yes
Calculate Results At	All Time Points
Analysis Data Management	
Solver Files Directory	C:\Documents and Settings\Administrator\Desktop\Solidworks\TOETSE\Models for evaluation of nozzle geometry\Nozzle geometry 3\Nozzle 3_files\dp0\SYS\MECH\
Future Analysis	None
Scratch Solver Files Directory	
Save MAPDL db	No
Delete Unneeded Files	Yes
Nonlinear Solution	No
Solver Units	Active System
Solver Unit System	mks

TABLE 13
Model (A4) > Steady-State Thermal (A5) > Loads

Object Name	*Heat Flow*	*Heat Flow 2*	*Heat Flow 3*	*Heat Flow 4*	*Convection*
State	Fully Defined				
Scope					
Scoping Method	Geometry Selection				
Geometry	1 Face		3 Faces	2 Faces	3 Faces
Definition					
Type	Perfectly Insulated				Convection
Define As	Perfect Insulation				
Magnitude	0. W				
Suppressed	No				
Film Coefficient					90. W/m^2·°C (ramped)
Ambient Temperature					-243. °C (ramped)

TABLE 15
Model (A4) > Steady-State Thermal (A5) > Loads

Object Name	*Temperature*	*Convection 2*
State	Fully Defined	
Scope		
Scoping Method	Geometry Selection	
Geometry	3 Faces	9 Faces
Definition		
Type	Temperature	Convection
Magnitude	26. °C (ramped)	
Suppressed	No	
Film Coefficient		20. W/m^2·°C (ramped)
Ambient Temperature		26. °C (ramped)

Solution (A6)

TABLE 17
Model (A4) > Steady-State Thermal (A5) > Solution

Object Name	*Solution (A6)*
State	Solved
Adaptive Mesh Refinement	
Max Refinement Loops	1.
Refinement Depth	2.
Information	
Status	Done

TABLE 18
Model (A4) > Steady-State Thermal (A5) > Solution (A6) > Solution Information

Object Name	*Solution Information*
State	Solved
Solution Information	
Solution Output	Solver Output
Update Interval	2.5 s
Display Points	All

TABLE 19
Model (A4) > Steady-State Thermal (A5) > Solution (A6) > Results

Object Name	*Temperature*	*Total Heat Flux*	*Directional Heat*

			Flux
State	Solved		
Scope			
Scoping Method	Geometry Selection		
Geometry	All Bodies		
Definition			
Type	Temperature	Total Heat Flux	Directional Heat Flux
By	Time		
Display Time	Last		
Calculate Time History	Yes		
Identifier			
Orientation			X Axis
Coordinate System			Global Coordinate System
Results			
Minimum	-242.99 °C	1.4997e-002 W/m²	-952.16 W/m²
Maximum	26.1 °C	15182 W/m²	15180 W/m²
Minimum Occurs On	Inner cylinder no extraction nozzle 3 (1)-1	Outer cylinder no extraction nozzle 3 (2)-1	Extraction nozzle 3-1
Maximum Occurs On	Vacuum no extraction nozzle 3-1	Extraction nozzle 3-1	
Information			
Time	1. s		
Load Step	1		
Substep	1		
Iteration Number	1		
Integration Point Results			
Display Option		Averaged	

TABLE 20
Model (A4) > Steady-State Thermal (A5) > Solution (A6) > Probes

Object Name	*Reaction Probe*
State	Solved
Definition	
Type	Reaction
Location Method	Boundary Condition
Boundary Condition	Convection
Options	
Display Time	End Time
Results	
Heat	-0.5733 W
Maximum Value Over Time	
Heat	-0.5733 W
Minimum Value Over Time	
Heat	-0.5733 W
Information	
Time	1. s
Load Step	1
Substep	1
Iteration Number	1

Material Data

Nozzle material

TABLE 21
Nozzle material > Constants

Thermal Conductivity	5 W m^-1 C^-1

Structural Steel

TABLE 22
Structural Steel > Constants

Density	7850 kg m^-3
Coefficient of Thermal Expansion	1.2e-005 C^-1
Specific Heat	434 J kg^-1 C^-1
Thermal Conductivity	16 W m^-1 C^-1
Resistivity	1.7e-007 ohm m

TABLE 23
Structural Steel > Compressive Ultimate Strength

Compressive Ultimate Strength Pa
0

TABLE 24
Structural Steel > Compressive Yield Strength

Compressive Yield Strength Pa
2.5e+008

TABLE 25
Structural Steel > Tensile Yield Strength

Tensile Yield Strength Pa
2.5e+008

TABLE 26
Structural Steel > Tensile Ultimate Strength

Tensile Ultimate Strength Pa
4.6e+008

TABLE 27
Structural Steel > Isotropic Secant Coefficient of Thermal Expansion

Reference Temperature C
22

TABLE 28
Structural Steel > Alternating Stress Mean Stress

Alternating Stress Pa	Cycles	Mean Stress Pa

3.999e+009	10	0
2.827e+009	20	0
1.896e+009	50	0
1.413e+009	100	0
1.069e+009	200	0
4.41e+008	2000	0
2.62e+008	10000	0
2.14e+008	20000	0
1.38e+008	1.e+005	0
1.14e+008	2.e+005	0
8.62e+007	1.e+006	0

TABLE 29
Structural Steel > Strain-Life Parameters

Strength Coefficient Pa	Strength Exponent	Ductility Coefficient	Ductility Exponent	Cyclic Strength Coefficient Pa	Cyclic Strain Hardening Exponent
9.2e+008	-0.106	0.213	-0.47	1.e+009	0.2

TABLE 30
Structural Steel > Isotropic Elasticity

Temperature C	Young's Modulus Pa	Poisson's Ratio	Bulk Modulus Pa	Shear Modulus Pa
	2.e+011	0.3	1.6667e+011	7.6923e+010

TABLE 31
Structural Steel > Isotropic Relative Permeability

Relative Permeability
10000

Vacuum

TABLE 32
Vacuum > Constants

Thermal Conductivity	2.e-004 W m^-1 C^-1

Appendix C: Manual calculations

Manual (EES) calculations and solutions

The manual calculations done are displayed followed by the results as given by EES. Appendix C is divided into two sections. In section one code, calculations and results about the base model are given. This is the method used for solving all heat transfer, boil-off, equivalent effects and graphical problems.

In section two code, calculations and results in terms of an acceptable boil-off are shown.

EES calculations and solutions: Code Section 1

```
"#######################Steady state thermal analysis###########################"
"#######################Cryogenic storage vessel###############################"

"#######################CYLINDER SYSTEM##############################"

"The cylinder system analyzed consist (from inside out) of the liquid hydrogen, the inner cylinder,
the vacuum, outer cylinder and ambient air."

"----------------------------Determining the size of tank to be analyzed--------------------------------------------"
"A comparison between a gasoline and cryogenic hydrogen tank will be used to determine the required
hydrogen cryogenic tank capacity."

"Energy capacities of gasoline and liquid hydrogen"
Energy_capacity_gas_per_kg = 44.4 [MJ/kg]
Energy_capacity_liq_hyd_per_kg = 144 [MJ/kg]

"Density of gasoline and liquid hydrogen"
Density_gasoline = 720 [kg/m^3]
Density_liq_hydrogen = 70 [kg/m^3]

"Determine the mass of 1kg liq hydrogen and gasoline"
Mass_1_literGasoline = Density_gasoline/1000
Mass_1_literLiqHyd = Density_liq_hydrogen/1000

"Calculate the energy in 1 liter of fuel"
Energy_in_1_l_gasoline = Mass_1_literGasoline*Energy_capacity_gas_per_kg
Energy_in_1_l_liq_hydrogen = Mass_1_literLiqHyd*Energy_capacity_liq_hyd_per_kg

"Use volume calculaters to determine the inner radius required"
"Assume that the energy required from the tank is 700 MJ. This is based on the fact that two of these
tanks are about equivilant to a gasoline tank of 45liter in terms of available energy"

Energy_req = 700 [MJ]

Total_mass_liq_hydrogen = Energy_req/Energy_capacity_liq_hyd_per_kg

Total_volume = Total_mass_liq_hydrogen/Density_liq_hydrogen
```

```
"Assume that the cryogenic hydrogen storage tank can be divided into two part namely a cylinder and a sphere."

Total_volume = Volume_sphere + Volume_cylinder

Volume_sphere = 4/3*PI*r_1^3                    "Determine inner radius of inner cylinder"
Volume_cylinder = PI*r_1^2*L

Tank_capacity = Total_volume*1000 [liter]       "Determine tank size"

"------------------------------Material properties, constants and conditions-------------------------------------"

"Length of cylinder"
L = 0.8                                          "Length of cylinder"

"Various radii of components"
r_2 = r_1 + 0.003                                "Outer radius of inner cylinder"
r_3 = r_2 + 0.1                                  "Inner radius of outer cylinder"
r_4 = r_3 + 0.003                                "Outer radius of outer cylinder"

"Thermal constants:"
"Convection constants"
k_InnerCylinder = 16                             "Boltzmann's constant for inner cylinder"

k_Insulation[1] = 0.0001                         "Boltzmann's constant for insulation"
k_Insulation[2] = 0.0003
k_Insulation[3] = 0.0005
k_Insulation[4] = 0.0007
k_Insulation[5] = 0.0009
k_Insulation[6] = 0.0011
k_Insulation[7] = 0.0013
k_Insulation[8] = 0.0015
k_Insulation[9] = 0.0017
k_Insulation[10] = 0.0019
k_OuterCylinder = 16                             "Boltzmann's constant for outer cylinder"

"Convection constants"
h_1 = 90  [W/m^2K]                               "Plank's constant for liquid hydrogen"
h_4 = 20  [W/m^2K]                               "Plank's constant for ambient air"

"Boundary temperatures"
T_1 = 20 [K]                                     "Liquid hydrogen temperature"
T_4 = 300 [K]                                    "Ambient air temperature"

"Latent heat of vaporization of liquid hydrogen"
h_fg = 44600 [J/kg]

"------------------------------Calculation of insulation and radiant barriers-------------------------------------"

"Insulation barrier value for inner cylinder"
R_InnerCylinder = t_InnerCylinder/k_InnerCylinder
 t_InnerCylinder = r_2 - r_1
Film_CoeffecientInner = 1/R_InnerCylinder

"Insulation barrier value for outer cylinder"
R_OuterCylinder = t_OuterCylinder/k_OuterCylinder
 t_OuterCylinder = r_4 - r_3
Film_CoeffecientOuter = 1/R_OuterCylinder
```

```
"Insulation barrier value for vacuum"
R_Vacuum = t_Vacuum/k_Insulation[3]
 t_Vacuum = r_3 - r_2
Film_CoeffecientVac = 1/R_Vacuum

"-------------------------------          Calculation of heat transfer          -------------------------------------"

"For radial conduction in a cylindrical wall, the thermal resistance is given by:"
"R_t,conduc = (ln(r_1/r_2))/(2*PI*L*k)"

"For radial convection in a cylindrical wall, the thermal resistance is given by:"
"R_t,convec = 1/(2*h*PI*r_1*L)"

"Thus the total heat transfer rate in the cylinder is:"

Duplicate i=1,10
q_rCylinder[i] = -1*(T_1 - T_4)/((1/(2*PI*L*r_1*h_1)) + ((ln(r_2/r_1))/(2*PI*L*k_InnerCylinder)) +
((ln(r_3/r_2))/(2*PI*L*k_Insulation[i])) + ((ln(r_4/r_3))/(2*PI*L*k_OuterCylinder)) + (1/(2*PI*L*r_4*h_4)))
end

"#######################SPHERE SYSTEM##############################"

"For the sphere, the same material properties, constants and conditions is considered"

"For radial conduction in a sphere wall, the thermal resistance is given by:"
"R_t,conduc = (1/(4*PI*k))*(1/r_1 - 1/r_2)"

"For radial convection in a sphere wall, the thermal resistance is given by"
"R_t,conduc = (1/h*4*PI*r^2)"


"Thus the total heat transfer rate in the Sphere is:"
Duplicate i=1, 10
q_rSphere[i] = -1*(T_1 - T_4)/((1/(h_1*4*PI*r_1^2)) + (1/(4*PI*k_InnerCylinder)*(1/r_1 - 1/r_2)) +
(1/(4*PI*k_Insulation[i])*(1/r_2 - 1/r_3)) + (1/(4*PI*k_OuterCylinder)*(1/r_3 - 1/r_4)) +
(1/(h_4*4*PI*r_4^2)))

"Total heat flow into the inner storage tank is:"
q_total[i] = (q_rSphere[i] + q_rCylinder[i])

"#######################ENERGY BALANCE##############################"
"Performing an energy balance on the system:"

"E_in = E_out"

E_in[i] = E_out[i]

E_in[i] = q_total[i]

"The loss of latent heat due to boiling can be expressed as m_dot*h_fg"

E_out[i] = m_dot_hydrogenPerSecond[i]*h_fg
m_dot_hydrogenPerhour[i] = m_dot_hydrogenPerSecond[i]*3600
m_dot_hydrogenPerDay[i] = m_dot_hydrogenPerhour[i]*24

Loss_of_energyPerHour[i] = m_dot_hydrogenPerhour[i]*Energy_capacity_liq_hyd_per_kg
Loss_of_energyPerHour[i] = Mass_GasLostPerHour[i]*Energy_capacity_gas_per_kg
Eq_l_GasLostPerHour[i] = Mass_GasLostPerHour[i]/(Density_gasoline/1000)
Eq_l_GasLostPerDay[i] = Eq_l_GasLostPerHour[i]*24
Eq_l_GasLostPerSecond[i] = Eq_l_GasLostPerHour[i]/3600
```

end

EES calculations and solutions: Solution section 1

Unit Settings: SI C kPa kJ mass deg

$Density_{gasoline}$ = 720 [kg/m^3]

$Density_{liq,hydrogen}$ = 70 [kg/m^3]

$Energy_{in,1,l,gasoline}$ = 31.97 [MJ]

$Energy_{in,1,l,liq,hydrogen}$ = 10.08 [MJ]

$Film_{CoeffecientOuter}$ = 5333 [W/m^2 K]

$Film_{CoeffecientVac}$ = 0.005 [W/m^2 K]

h_{fg} = 44600 [J/kg]

$k_{InnerCylinder}$ = 16 [W/mK]

$Mass_{1,literGasoline}$ = 0.72 [kg]

$Mass_{1,literLiqHyd}$ = 0.07 [kg]

r_3 = 0.2518 [m]

r_4 = 0.2548 [m]

R_{Vacuum} = 200 [W/mm^2]

$Tank_{capacity}$ = 69.44 [liter]

T_1 = 20 [K]

T_4 = 300 [K]

t_{Vacuum} = 0.1 [m]

$Volume_{cylinder}$ = 0.05564 [m^3]

$Energy_{capacity,gas,per,kg}$ = 44.4 [MJ/kg]

$Energy_{capacity,liq,hyd,per,kg}$ = 144 [MJ/kg]

$Energy_{req}$ = 700 [MJ]

$Film_{CoeffecientInner}$ = 5333 [W/m^2 K]

h_1 = 90 [W/m^{2}K]

h_4 = 20 [W/m^{2}K]

$k_{OuterCylinder}$ = 16 [W/mK]

L = 0.8 [m]

r_1 = 0.1488 [m]

r_2 = 0.1518 [m]

$R_{InnerCylinder}$ = 0.0001875 [W/mm^2]

$R_{OuterCylinder}$ = 0.0001875 [W/mm^2]

$Total_{mass,liq,hydrogen}$ = 4.861 [kg]

$Total_{volume}$ = 0.06944 [m^3]

$t_{InnerCylinder}$ = 0.003 [m]

$t_{OuterCylinder}$ = 0.003 [m]

$Volume_{sphere}$ = 0.0138 [m^3]

Sort	1 $k_{Insulation,i}$ [W/mK]	2 $E_{in,i}$ [W]	3 $E_{out,i}$ [W]	4 $m_{hydrogenPerDay i}$ [kg/day]	5 $m_{hydrogenPerhour i}$ [kg/h]	6 $m_{hydrogenPerSecond i}$ [kg/s]	7 $q_{rSphere,i}$ [W]	8 $q_{rCylinder,i}$ [W]
[1]	0.0001	0.4126	0.4126	0.7992	0.0333	0.00000925	0.1345	0.2781
[2]	0.0003	1.238	1.238	2.398	0.0999	0.00002775	0.4034	0.8342
[3]	0.0005	2.062	2.062	3.995	0.1665	0.00004624	0.6723	1.39
[4]	0.0007	2.887	2.887	5.593	0.233	0.00006474	0.9412	1.946
[5]	0.0009	3.712	3.712	7.191	0.2996	0.00008322	1.21	2.502
[6]	0.0011	4.536	4.536	8.788	0.3662	0.0001017	1.479	3.057
[7]	0.0013	5.36	5.36	10.38	0.4327	0.0001202	1.748	3.613
[8]	0.0015	6.185	6.185	11.98	0.4992	0.0001387	2.016	4.168
[9]	0.0017	7.009	7.009	13.58	0.5657	0.0001571	2.285	4.723
[10]	0.0019	7.832	7.832	15.17	0.6322	0.0001756	2.554	5.279

9 $q_{total,i}$ [W]	10 $Loss_{of,energyPerHour}$ [MJ]	11 $Mass_{GasLostPerHour}$ [kg]	12 $Eq_{l,GasLostPerDay}$ [liter]	13 $Eq_{l,GasLostPerHour}$ [liter]	14 $Eq_{l,GasLostPerSecond}$ [liter]
0.4126	4.795	0.108	3.6	0.15	0.00004167
1.238	14.39	0.324	10.8	0.45	0.000125
2.062	23.97	0.5399	18	0.7499	0.0002083
2.887	33.56	0.7558	25.19	1.05	0.0002916
3.712	43.14	0.9717	32.39	1.35	0.0003749
4.536	52.73	1.188	39.58	1.649	0.0004581
5.36	62.31	1.403	46.78	1.949	0.0005414
6.185	71.89	1.619	53.97	2.249	0.0006246
7.009	81.46	1.835	61.16	2.548	0.0007078
7.832	91.04	2.05	68.35	2.848	0.0007911

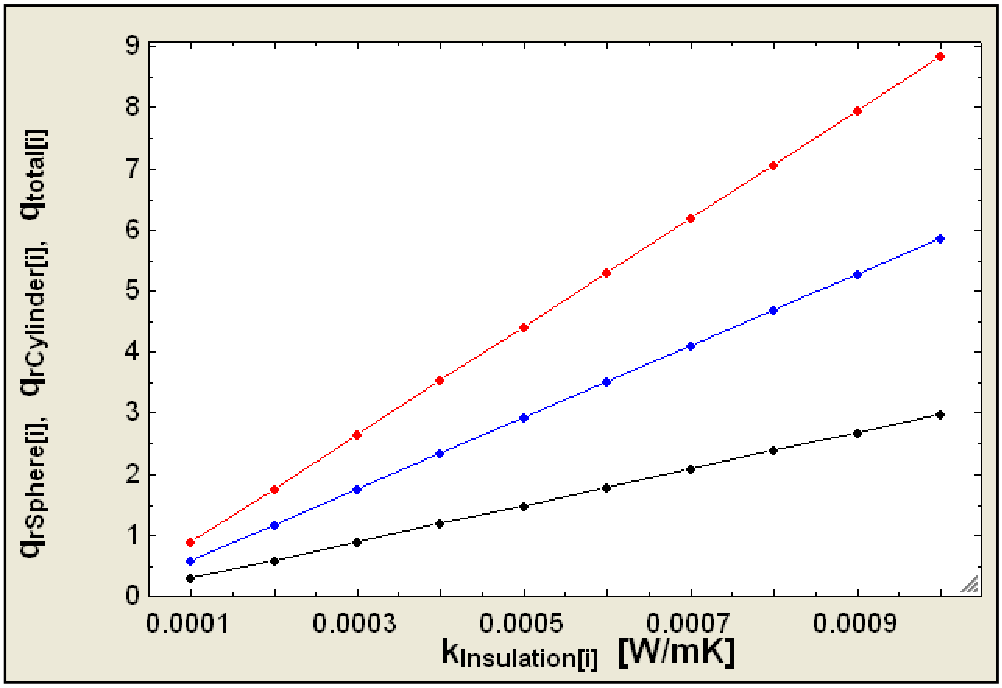

Figure 27: A comparison between the amounts of heat transferred for different areas of the system.

EES calculations and solutions: Code Section 2

```
"################CALCULATION of acceptable boil-off#####################"

"Energy capacities of gasoline and liquid hydrogen"
Energy_capacity_gas_per_kg = 44.4 [MJ/kg]
Energy_capacity_liq_hyd_per_kg = 144 [MJ/kg]

"Density of gasoline and liquid hydrogen"
Density_gasoline = 720 [kg/m^3]
Density_liq_hydrogen = 70 [kg/m^3]

"Determine the mass of 1kg liq hydrogen and gasoline"
Mass_1_literGasoline = Density_gasoline/1000
Mass_1_literLiqHyd = Density_liq_hydrogen/1000

"Calculate the energy in 1 liter of fuel"
Energy_in_1_l_gasoline = Mass_1_literGasoline*Energy_capacity_gas_per_kg
Energy_in_1_l_liq_hydrogen = Mass_1_literLiqHyd*Energy_capacity_liq_hyd_per_kg


"Determine the amount of energy used per day by a vehicle"
Average_driving_distance = 54 [km per day]

Vehicle_fuel_consumption_rate = 15 [km/liter_gasoline]

Gasoline_consumption_per_day = Average_driving_distance/Vehicle_fuel_consumption_rate

Energy_used_per_day = Gasoline_consumption_per_day*Energy_in_1_l_gasoline

"Determine the amount hydrogen that will be consumed on an average driving day"

"Hydrogen consumption per day in liter:"
Energy_used_per_day = Hydrogen_consumption_per_day*Energy_in_1_l_liq_hydrogen

Volume_hydrogen_consumed_daily = Hydrogen_consumption_per_day/1000

Mass_hydrogen_consumed_daily = Density_liq_hydrogen*Volume_hydrogen_consumed_daily

"Determine the acceptable boil-off"

Acceptable_Boil_off = Mass_hydrogen_consumed_daily
```

Unit Settings: SI C kPa kJ mass deg

$Acceptable_{Boil,off}$ = 0.7992 [kg/day]

$Density_{liq,hydrogen}$ = 70 [kg/m^3]

$Energy_{in,1,l,gasoline}$ = 31.97 [MJ/liter]

$Gasoline_{consumption,per,day}$ = 3.6 [liter]

$Mass_{1,literLiqHyd}$ = 0.07 [kg]

$Volume_{hydrogen,consumed,daily}$ = 0.01142 [m^3]

$Average_{driving,distance}$ = 54 [km·per·day]

$Energy_{capacity,gas,per,kg}$ = 44.4 [MJ/kg]

$Energy_{in,1,l,liq,hydrogen}$ = 10.08 [MJ/liter]

$Hydrogen_{consumption,per,day}$ = 11.42 [liter]

$Mass_{hydrogen,consumed,daily}$ = 0.7992 [kg]

$Density_{gasoline}$ = 720 [kg/m^3]

$Energy_{capacity,liq,hyd,per,kg}$ = 144 [MJ/kg]

$Energy_{used,per,day}$ = 115.1 [MJ]

$Mass_{1,literGasoline}$ = 0.72 [kg]

$Vehicle_{fuel,consumption,rate}$ = 15 [km/liter$_{gasoline}$]

Appendix D: CES selection

Cambridge Engineering Selector procedure and results

In this appendix the process used to select the thermal conductivity of the nozzle material is explained. CES (Cambridge Engineering Selector) was used assist in the selection of this value.

For this selection the CES analysis consisted of using a process of two dimensional filtering. The criteria used for two dimensional filtering for this selection were service temperature and thermal expansion. As observed in a graphical representation of the analysis in Figure 28, materials are displayed graphically after two dimensional filtering with the property minimum service temperature labeled on the x-axis, while the y-axis gives the materials thermal expansion.

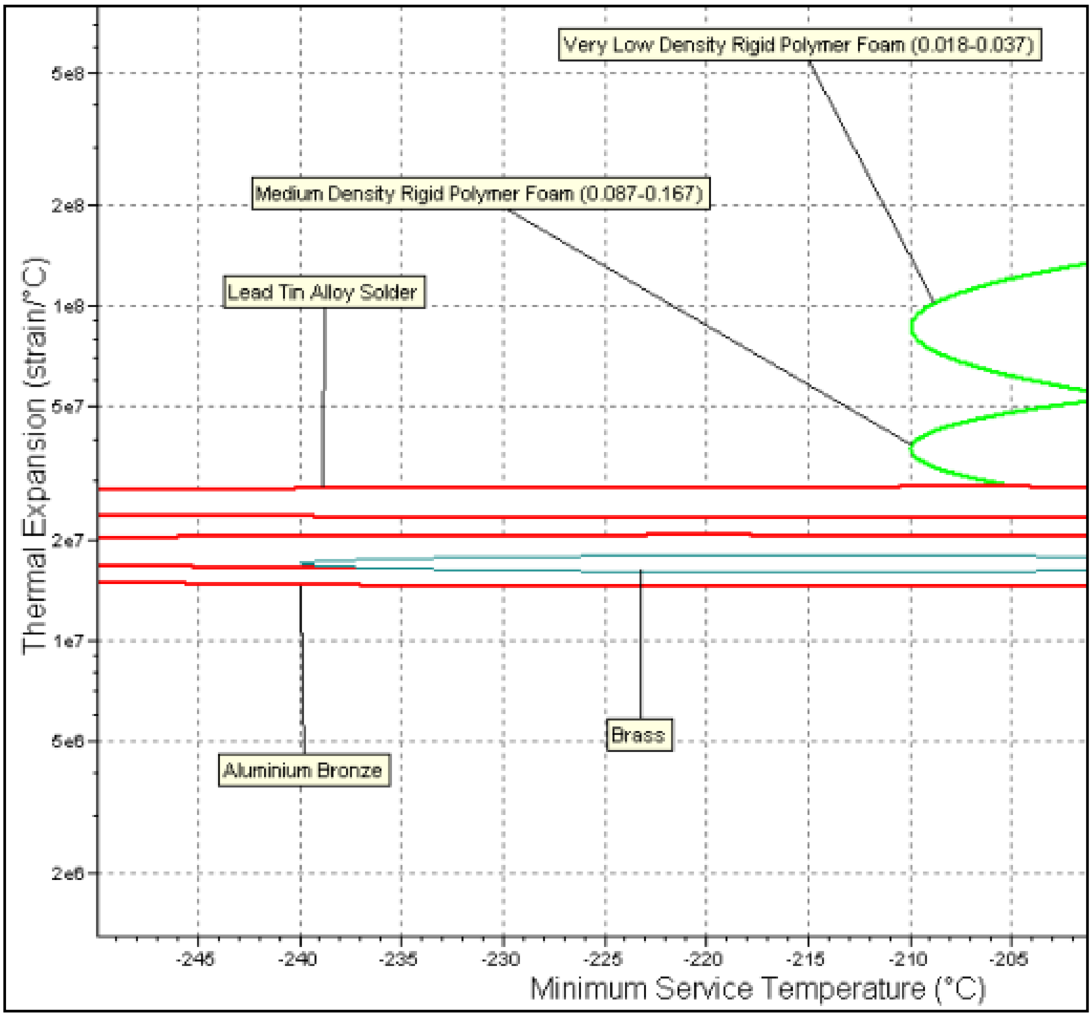

Figure 28: A graphical representation of the interface of CES.

Together with thermal conductivity, these two properties formed the base for selection of the nozzle material. The filtering process used in CES eliminated all materials that cold not operate below -205°C. It also filtered out materials with a high thermal expansion (above 2e8 strain/°C). The properties of the five materials selected by the filtering process are given in Table 15.

Table 15: The potential materials used for the nozzle as filtered out by CES.

Material	Min service temperature [°C]	Min thermal conductivity [W/mK]	Thermal expansion [strain/°C]
Lead tin alloy solder	-273	35	2.30E+07
Aluminium Bronze	-270	60	1.45E+07
Brass	-273	110	1.65E+07
Very low density rigid polymer foam	-210	0.019	3.40E+07
Medium density rigid polymer foam	-210	0.027	2.00E+07

- From the considered materials the most important property is thermal conductivity. However, the minimum service temperature and thermal expansion also plays a significant part. Large thermal expansions may lead to hydrogen gas leaking past the nozzle and into the vacuum, compromising the total system.
- A significant drawback of polymer foams is its mechanical properties, since its bulk modulus is only 4 MPa.
- In terms of the lead tin alloy solder, it shows the lowest thermal conductivity of the other three materials, but it has it has a thermal expansion value of almost double that of aluminum bronze and brass. For that reason it was not considered in the decision for the thermal conductivity of the nozzle.

The calculations and assumptions used to obtain the thermal conductivity of the nozzle were as follows:

- It was calculated that the average thermal conductivity between *lead tin alloy solder* and *aluminum bronze* was 31.667 W/mK. It was also calculated that the average between the thermal conductivity of very low density rigid polymer foam and medium density rigid polymer foam was 0.023 W/mK.
- It was assumed that a very well insulated nozzle would compose of about 15% structural element, while the other 85% of the material would be used for insulation.

Based on this, the following equation was used to calculate the thermal conductivity of the nozzle:

$$\left(\frac{15}{100}\ X\ 31.667\ W/mK\right) + \left(\frac{85}{100}\ X\ 0.023\ W/mK\right) = 4.77\ W/mK$$

- The thermal conductivity value used for the nozzle was 5 W/mK.